MASTER IN CHEMISTRY PROFESSIONAL FOCUS

Synthesis of aziridines as potential inactivators of GlfH1, a novel glycosidase from Mycobacterium tuberculosis

PIRARD, François

Award date:
2023

Awarding institution:
University of Namur

Université de Namur

Faculté des Sciences

SYNTHESIS OF AZIRIDINES AS POTENTIAL INHIBITORS OF GLfH1, A NOVEL GLYCOSIDASE FROM *MYCOBACTERIUM TUBERCULOSIS*

Mémoire présenté pour l'obtention

du grade académique de Master Chimie « Chimie du vivant et des nanomatériaux » : Finalité Spécialisée

François PIRARD

Janvier 2023

« When the world is in trouble,
chemistry comes to the rescue »

Carolyn R. Bertozzi

UNIVERSITE DE NAMUR
Faculté des Sciences
Secrétariat du Département de Chimie
Rue de Bruxelles 61 – 5000 NAMUR
Téléphone : +32(0)81 72.54.44 – Téléfax : +32(0)81 72.54.40 E-mail : enseignement.chimie@unamur.be - www.unamur.be/sciences

Synthesis of aziridines as potential inactivators of Gl*f*H1, a novel glycosidase from *Mycobacterium tuberculosis*

PIRARD François

Résumé

La tuberculose est une maladie pulmonaire causée par *Mycobacterium tuberculosis*, un agent pathogène bactérien. Cette infection touche 25% de la population mondiale et constitue la 13ème cause de mortalité. Avec l'émergence de nouvelles résistances aux traitements antibiotiques standards, il est crucial de développer de nouvelles thérapies.

La découverte de Gl*f*H1, une galactofuranosidase impliquée dans la dégradation de la paroi cellulaire des mycobactéries, a conduit au développement d'une nouvelle cible thérapeutique potentielle. Le rôle de Gl*f*H1, une *exo*-β-D-galactofuranosidase, est de cliver les résidus galactofuranosyl terminaux de la chaîne galactane présente dans le complexe arabinogalactane de la paroi cellulaire mycobactérienne. Le mécanisme de Gl*f*H1 est basé sur une catalyse covalente, entraînant la rétention de la configuration en position anomérique. La formation de l'intermédiaire covalent généré par ce type de mécanisme est la clé pour obtenir une inhibition irréversible de cette glycosidase. Il a été démontré que les glycomimétiques porteurs de groupements aziridines peuvent potentiellement avoir un fort effet inhibiteur grâce à leur réactivité particulière combinant une forte tension de cycle et un important caractère électrophile et cationique pour mimer l'état de transition.

Pour inhiber Gl*f*H1, une approche potentielle consiste à synthétiser un glycomimétique d'un résidu galactofuranosyl porteur d'une aziridine. La stratégie mise en place consiste à synthétiser cette aziridine à partir d'un précurseur cyclopentene réalisé à partir du D-Galactose. La synthèse de ce précurseur cyclopentene a pu être réalisée avec succès avec un rendement global de 4% sur huit étapes. Cependant, la mise en place de l'aziridine n'a pas pu être réalisé avec succès.

Mémoire de master en Sciences Chimiques à Finalité Spécialisée

Janvier 2023

Promoteur : Professeur VINCENT

UNIVERSITE DE NAMUR
Faculté des Sciences
Secrétariat du Département de Chimie
Rue de Bruxelles 61 – 5000 NAMUR
Téléphone : +32(0)81 72.54.44 – Téléfax : +32(0)81 72.54.40 E-mail : enseignement.chimie@unamur.be - www.unamur.be/sciences

Synthesis of aziridines as potential inactivators of Gl*f*H1, a novel glycosidase from *Mycobacterium tuberculosis*

PIRARD François

Overzicht

Tuberculose is een longziekte die wordt veroorzaakt door *Mycobacterium tuberculosis*, een bacteriële ziekteverwekker. De infectie treft 25% van de wereldbevolking en is de dertiende doodsoorzaak. Met het ontstaan van nieuwe resistenties tegen standaard antibioticabehandelingen is het van cruciaal belang nieuwe therapieën te ontwikkelen.

De ontdekking van Gl*f*H1, een galactofuranosidase dat betrokken is bij de afbraak van de mycobacteriële celwand, heeft geleid tot de ontwikkeling van een potentieel nieuw therapeutisch doelwit. De rol van Gl*f*H1, een *exo*-β-D-galactofuranosidase, bestaat erin de galactofuranosyl residuen van de galactanketen in het arabinogalactancomplex van de mycobacteriële celwand te splijten. Het mechanisme van Gl*f*H1 is gebaseerd op covalente katalyse, wat resulteert in het behoud van de configuratie op de anomere positie. De vorming van het covalente tussenproduct dat door dit soort mechanisme wordt gegenereerd, is de sleutel tot het bereiken van onomkeerbare remming van deze glycosidase. Gebleken is dat glycomimetica met aziridine groepen potentieel een sterk remmend effect kunnen hebben door hun bijzondere reactiviteit waarbij een hoge ringspanning en een hoog elektrofiel en kationisch karakter worden gecombineerd om de overgangstoestand na te bootsen.

Om Gl*f*H1 te remmen is een mogelijke aanpak de synthese van een glycomimetisch galactofuranosyl residu met een aziridine. De toegepaste strategie bestaat uit de synthese van dit aziridine uit een cyclopentene precursor op basis van D-Galactose. De synthese van deze cyclopenteen-precursor werd met succes uitgevoerd met een totaalrendement van 4% in acht stappen. De vaststelling van aziridine was echter niet mogelijk.

Mémoire de master en Sciences Chimiques à Finalité Spécialisée

Janvier 2023

Promoteur : Professeur VINCENT

Remerciements

Je souhaite remercier, en premier lieu, le professeur Stéphane Vincent pour m'avoir accueilli au sein de son laboratoire et intégré au sein de son équipe. Le temps qu'il m'a accordé pour mes requêtes, répondre à mes questions, me donner des conseils avisés a largement contribué à la rédaction de ce mémoire

Je tiens également à remercier de tout cœur mon encadrant, Loïc Chêne, pour m'avoir accompagné au quotidien et aidé à mieux apprivoiser cette science à la fois capricieuse mais si fascinante. Je le remercie non seulement pour le temps qu'il m'a accordé au laboratoire mais aussi pour tous les bons moments passés en dehors de l'université et avec qui j'ai partagé beaucoup de souvenirs inoubliables. Je le félicite pour son récent titre de docteur amplement mérité.

Les membres du CBO n'étaient pas seulement des collègues de travail, ils sont devenus pour moi bien plus, comme une seconde famille avec qui j'ai partagé mon quotidien le temps d'une année. Je remercie Arnaud, Marine et Rym qui m'ont apporté tant de bons conseils, faisaient régner bonne humeur et convivialité au sein du labo et surtout m'ont beaucoup fait rire. Je remercie également Florence, Kévin, Jenny, Nacho, Dmytro, Léa, Jun, Thimothé, Maha et Giuseppe pour l'aide et le soutient qu'ils m'ont accordé sans compter l'accueil chaleureux qu'ils m'ont réservé.

De manière plus générale, j'exprimerai toute ma reconnaissance envers mes professeurs, mes assistants et mes camarades de master qui m'ont apporté tant de connaissances et de précieux conseils qui, indirectement, ont contribué à la réalisation de ce mémoire

Je n'oublierai pas de remercier mes colocataires Baptiste Duby et Marine Parent avec qui j'ai vécu au quotidien cette année de mémoire et qui m'ont soutenu tout au long de ce chemin. Ils ont si souvent montré leur intérêt à mon projet.

Je remercie aussi mes parents qui m'ont permis et encouragé à faire les études qui me plaisaient et à m'épanouir dans la vie universitaire.

Enfin, je remercie mes grands-parents qui n'ont malheureusement plus la chance d'être auprès de nous mais qui ont toujours été une source de motivation à tout point de vue et qui ont réussi à susciter chez moi ce désir de satisfaire cette curiosité grandissante, tant pour les sciences que pour tous les autres domaines.

Abbréviations

Å	Ångström
Ac	Acetyl
AG	Arabinogalactan
AGP	Arabinogalactan peptydoglycan
Ara*f*	Arabinofuranose
Bn	Benzyl group
COSY	Correlation spectroscopy
Cy	Cyclohexane
δ	Chemical shift
DCM	Dichloromethane
DIBAL-H	Di-isobutylaluminium hydride
equiv.	Equivalent
Et	Ethyl group
EtOAc	Ethyl acetate
Gal*f*	Galactofuranose
GH	Glycoside hydrolase
GlcNAc	*N*-Acetyl glucosamine
HIV	Human immunodeficiency virus
HMBC	Heteronuclear multiple bond correlation
HMQC	Heteronuclear quantum bond correlation
J	Coupling constant
m-CPBA	meta-chloroperbenzoique acid
MA	Mycolic acids
mAGP	Mycolil-arabinogalactan-peptydoglycan
MDR	Multi drug resistant
Me	Methyl group
MeCN	Acetonitrile
Mtb	*Mycobacterium tuberculosis*
Mur	Muramic acids
MurNAc	*N*-acetylmuramic acid
MurNGlc	*N*-glucolylmuramic acid
NMR	Nuclear magnetic resonance
nOe	Nuclear Overhauser effect
OBn	Benzyl ether group
PDR	Pandrug resistant
PG	Peptydoglycan
Ph	Phenyl group
pK_a	Acid dissociation constant
PPh_3	Triphenylphosphine
ppm	Part per million
pTsOH	Para toluene sulfonic acid
r.t.	Room temperature
R_f	Retention factor
TB	Tuberculosis
TLC	Thin layer chromatography
Ts	para toluene sulfonyl group
WHO	World Health Organization
XDR	Extended drug resistant

Table of content

I. INTRODUCTION

I.1. Tuberculosis

Tuberculosis (TB) is a disease that mainly affects the lungs but also other systems such as the lymphatic system, the central nervous system, the bones, the liver and the intestinal tract. Disease is caused by a pathogenic bacterium, *Mycobacterium tuberculosis* (*Mtb*), a bacterium of the bacillus family discovered by the German biologist Robert Koch in 1882.[1] In 2020, according to the World Health Organization (WHO), it was estimated that between one in four and one in five people in the world were contaminated by the bacterium causing, in the same year, nearly 9.9 million deaths.[2] Nearly two-thirds of new cases are concentrated in just eight countries: India, China, Pakistan, Bangladesh, South Africa, the Philippines, Nigeria and Indonesia. This unequal distribution can be explained by multiple factors such as the lack of access to medical infrastructures, malnutrition, precariousness or the presence of other epidemics like human immunodefficiency viruses (HIV)[2].

In addition to all these factors, *Mtb* develops new resistance to conventional antibiotics. Conventional treatments are based on the use of antibiotics such as pyrazinamide, ethambutol, isoniazid or rifampicin, but the appearance of new and increasingly resistant strains makes them less and less effective.[3–5] Resistances are classified in several groups according to the European Centre for Disease Control (ECDC) : Multidrug resistance (MDR), Extended drug resistance (XDR) and Pandrug resistant (PDR). MDR was defined as acquired non-susceptibility to at least one agent in three or more antimicrobial categories. XDR was defined as non-sensible to at least one agent in all but two or fewer antimicrobial categories (i.e., bacterial isolates remain sensible to only one or two antimicrobial categories). Finally PDR was defined as non suceptibility to all agents in antimicrobial categories.[6]

I.2. Infection cycle

TB is a communicable disease initiated by the inhalation of micro droplets emitted from the airways of infected persons when he cought or sneezes (**Figure 1**). These particles measure between 1 - 5 µm in diameter and can remain in air for up to several hours due to their small size.[7] The ID_{50} (minimum number of pathogenic agent required to infect 50% of population) is estimated to less than 10 bacilli for humans.[8] These droplets are then inhaled, and avoid, by their small size, the physiological barriers of the bronchi, causing them to clump together in the lungs *Mtb* is free to enter cells, phagocytic or not, within the pulmonary alveoli and to trigger

an immediate innate immune response responsible for the pulmonary inflammation. The increase in B lymphocytes and T lymphocytes activate macrophages and other leukocytes leading to the establishment of granulomas containing *Mtb*. Some people will eventually develop active disease, which can lead to the release of *Mtb* from these granulomas, which, when eroded, can re-enter into the airways and be re-emited when people with active TB cough. These people in turn produce infectious droplets that transmit the infection.

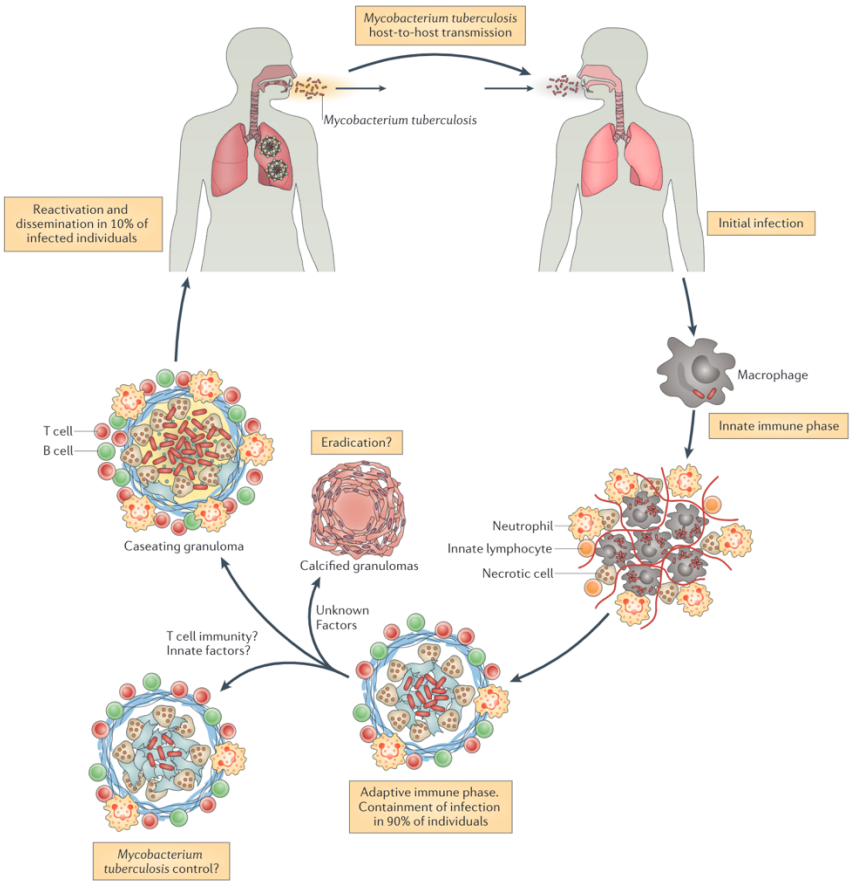

***Figure 1**. infection cycle of Mtb. Illustration issued from Nunes-Alves C. et al.*[9]

Most of the time, when infected, the immune system is fully capable of eliminating the pathogenic bacteria. In some cases, affected individuals develop a latent form of the disease, they are infected but do not develop signs of infection or contagiousness. At this stage, the bacteria may remain latent for the life of the individual or evolve into an active form with the onset of contagiousness, symptoms and disease. The emergence of this stage remains rare and concerns mainly fragile people and those considered at risk such as those suffering from diabetes or HIV.

I.3. Mycobacterium cell wall

Usually, bacteria can be classified into two categories: the so-called Gram-positive bacteria and the so-called Gram-negative bacteria. The majority of bacteria belong to one or the other of these two categories. Gram-positive bacteria have a phospholipid membrane protected by an outer cell wall rich in peptidoglycan, whereas Gram-negative bacteria have an inner phospholipid membrane, a thin layer of in peptidoglycan and an additional outer phospholipid membrane. (**Figure 2**).

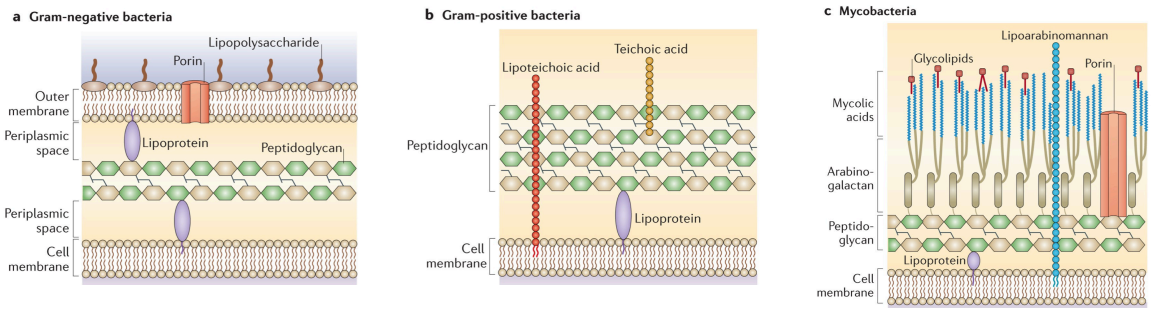

***Figure 2**. Gram negative bacterial, Gram positive bacterial and mycobacterial cell wall structure. Illustration taken from Brown L et al.*[10]

Unlike most bacteria, *Mtb* does not belong to either of these two categories because of the structural complexity of its bacterial cell wall. The main difference of the mycobacterial wall, compared to the other two walls, is its high proportion of lipids, making it particularly impermeable and resistant to hydrophilic substances. The mycobacterial wall is divided into three interconnected entities, the whole forming a single macromolecular structure (**Figure 3**). These three entities are :

- Peptidoglycan (PG)
- Arabinogalactan (AG)
- Mycolic acids (MA)

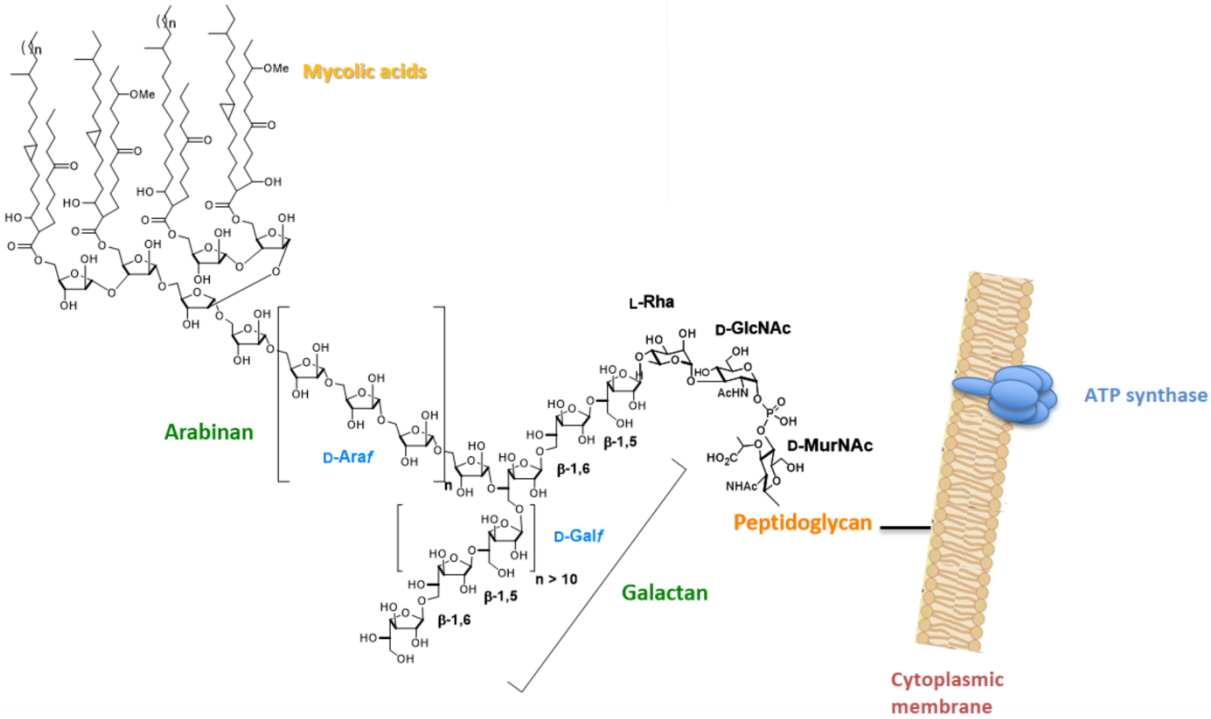

***Figure 3**. Structure of Mycobacterium tuberculosis cell wall.*

I.3.1. Peptidoglycan (PG)

Peptidoglycan is an essential component of the bacterial wall. Common to all bacteria, PG contributes to the maintenance of the integrity and the shape of the bacteria, any disruption of which would lead to cell lysis.[11] It also protects it from hydrostatic pressure phenomena such as turgidity. PG ensures other functions as an anchoring point for proteins or glycosidic chains.[12]

Its chemical composition consists of chains of linear and ß-linked glycosidic residues consisting of alternating *N*-acetylglucosamine **1** and muramic acid residues such as N-glucolylmuramic acid **2** and *N*-acetylmuramic acid **3 (Figure 4**).[12]

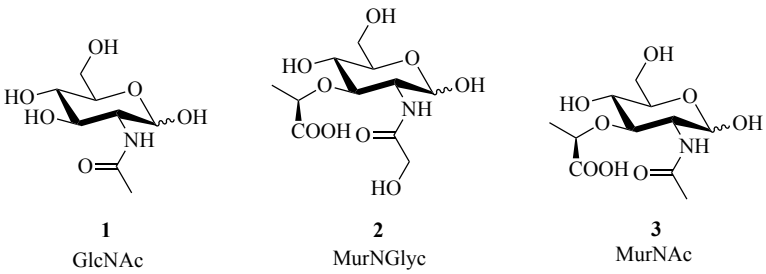

***Figure 4.** structure of glycosides constituents of PG.*

I.3.2. Mycolic acids (MA)

Mycolic acids form the outer layer of the mycobacterial cell wall. They are β-hydroxy fatty acids with a long α-alkyl side chain of high molecular weight with a carbon skeleton of 70 to 90 carbon atoms.[13] The whole representing up to 60% of the total dry mass of the bacteria.[14] The role of this hydrophobic bulwark is to confer to the bacteria a resistance to dehydration, the capacity to persist and grow in the hostile environment of the macrophage phagolysosome as well as a great impermeability to hydrophilic antibiotic substances, up to 1000 times less permeable to ß-lactam antibiotics than a Gram-negative bacterium.[15,16] The three classes of mycolic acids present in *Mtb* are listed in **Figure 5.**

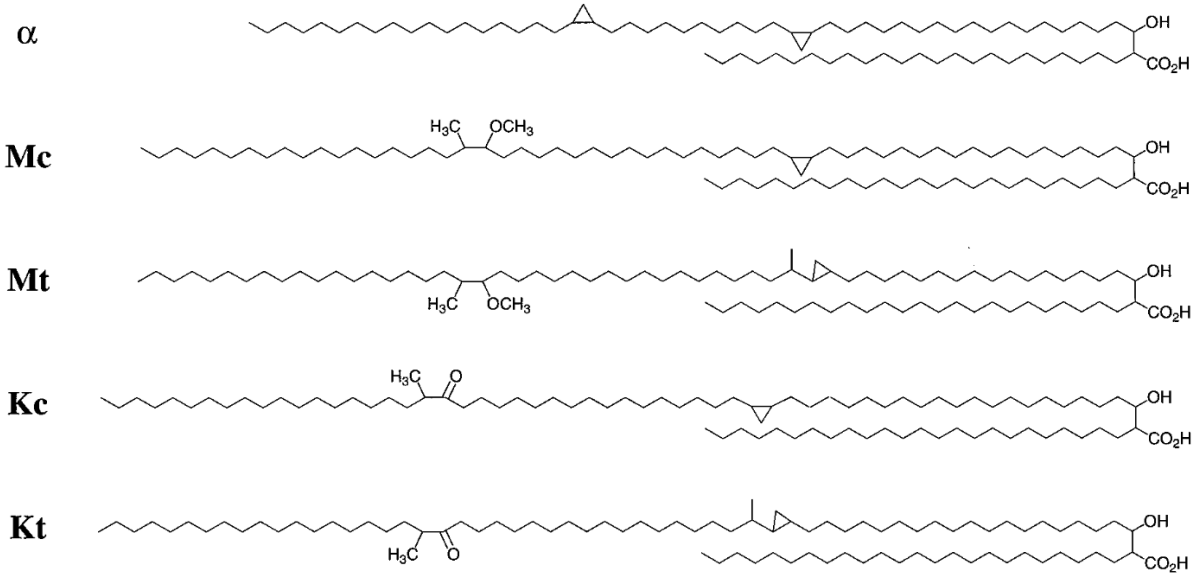

***Figure 5**. structure of Mycolic acids from Mycobacterium tuberculosis : α-mycolic acids, methoxymycolic acids cis-cyclopropane (Mc), methoxymycolic acids trans-cyclopropane (Mt), ketomycolic acids cis-cyclopropane (Kc) and ketomycolic acids trans-cyclopropane (Kt). Illustration taken from Yuan Y. et al.* [17]

I.3.3. Arabinogalactan (AG)

AG constitutes the intermediate layer of the mycobacterial wall, located between the mycolic acid layer and the peptidoglycan. It is a branched heteropolysaccharide consisting of two linked glycosidic chains: galactan and arabinan.[18]

- The galactan chain is a chain consisting in around thirty D-galactofuranosyl residues **4** alternately linked β (1 → 5) and β (1 → 6).
- The arabinan chain is a chain consisting in twenty-three predominantly α (1 → 5) linked D-arabinofuranosyl residues **5** with random α (1 → 3) linked branches. The junction with the galactan chain occurs on the 8th, 10th, and 12th D-Gal*f* residues.

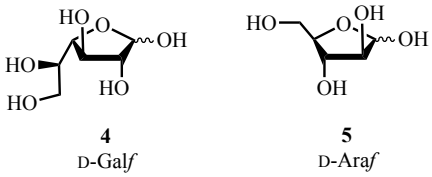

***Figure 6**. structure of D-Galf and D-Araf, constiuent of arabinogalactan chain.*

The end of the galactan chain connects the AG to the peptydoglycan via a link established by a disaccharide: L-Rhamnose **6** and D-N-acetylglucosamine **1** (**Figure 7).** The latter is attached to an N-acetylmuramic acid residue **3** of the PG by a phosphodiester bond.

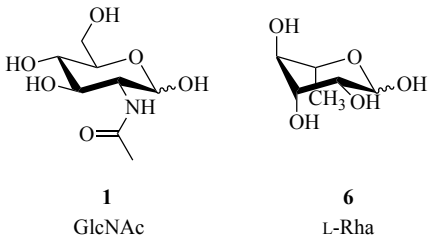

***Figure 7**. structure of GlcNAc and L-Rhap constituent the linker.*

The other end of the AG, is connected to the mycolic acids by an ester linkage established between the carboxylic acid of the mycolic acids and the non-reducing terminal position of the last arabinofuranose residue.

The galactofuranosyl units **4** forming the galactan chain are synthesized from a UDP-Gal*f* nucleoside precursor. This UDP-Gal*f* **9** unit is obtained from a UDP-Gul*p* precursor. First, the epimerization reaction of UDP-Glu*p* **7** catalyzed by a UDP-gluco-4-epimerase (GALE, Rv3634) allows the conversion to UDP-Gal*p* **8**. A second enzyme, UDP-galactopyranose mutase (UGM, Rv3809c) catalyzes the conversion of the pyranose form of UDP-Gal*p* **8** to the furanose form UDP-Gal*f* **9** (**Scheme 1**).[19]

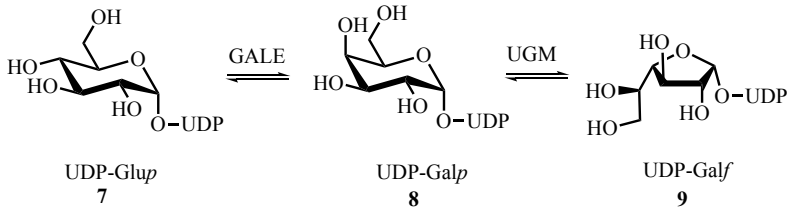

Scheme 1. biosynthesis of UDP-Galactofuranose (UDP-Galf)

These UDP-Gal*f* units form the galactofuranosyl residues of the galactan chain through two Galf transferases: Gl*f*T1 (Rv3782) and Gl*f*T2 (Rv3808c) (**Figure 8**). Initially, Gl*f*T1 transfers Galf from the UDP-Gal*f* to the C-4 position of L-Rha, then adds a second Gal*f* residue to the C-5 position of the primary Gal*f*. Then, Gl*f*T2 sequentially transfers Gal*f* residues to the growing galactan chain with alternating β(1 → 5) and β(1 → 6) glycosidic bonds.[20]

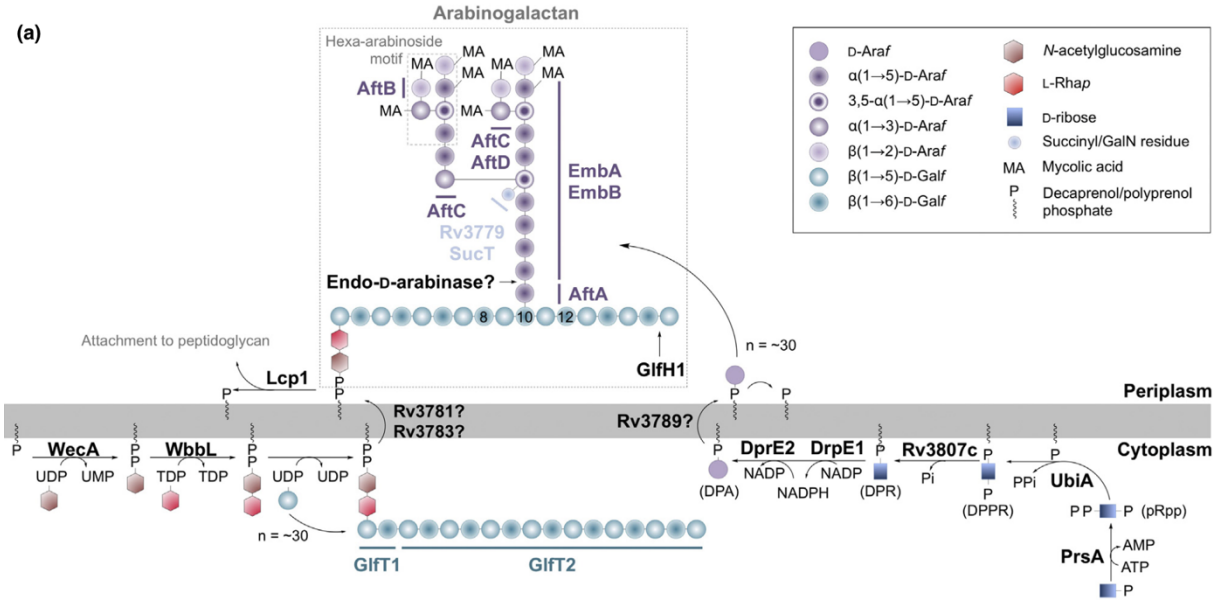

Figure 8. Biosynthesis of arabinogalactan, illustration isssued from Abraham K. et al.[13]

I.4. Cell wall remodeling

This structure of the *Mtb* cell wall is more complex as it is subject to different variations in shape and composition. These variations depend on multiple factors such as the stage of infection, a stress or a change in the environment of the bacterium and its stage of growth.[13] These variations allow *Mtb* to constantly remodel its wall thickness and composition to adapt to and cope with environmental stress conditions.

In its active form, there is an increase in the concentration and activity of peptidoglycan, arabinogalactan and mycolic acids in the cell wall (**Figure 9**). This results in a wall that is more

resistant to the environment and impermeable to hydrophilic substances, especially antibiotics, which facilitates its expansion. In stasis, *Mtb* grows more slowly and tends to decrease the abundance and activity of mycolic acids, peptidoglycan and arabinogalactan potentially to escape immune recognition. Similarly, peptidoglycan cross-linking may be increased to promote cell wall rigidity and bacterial survival under stress conditions.[19]

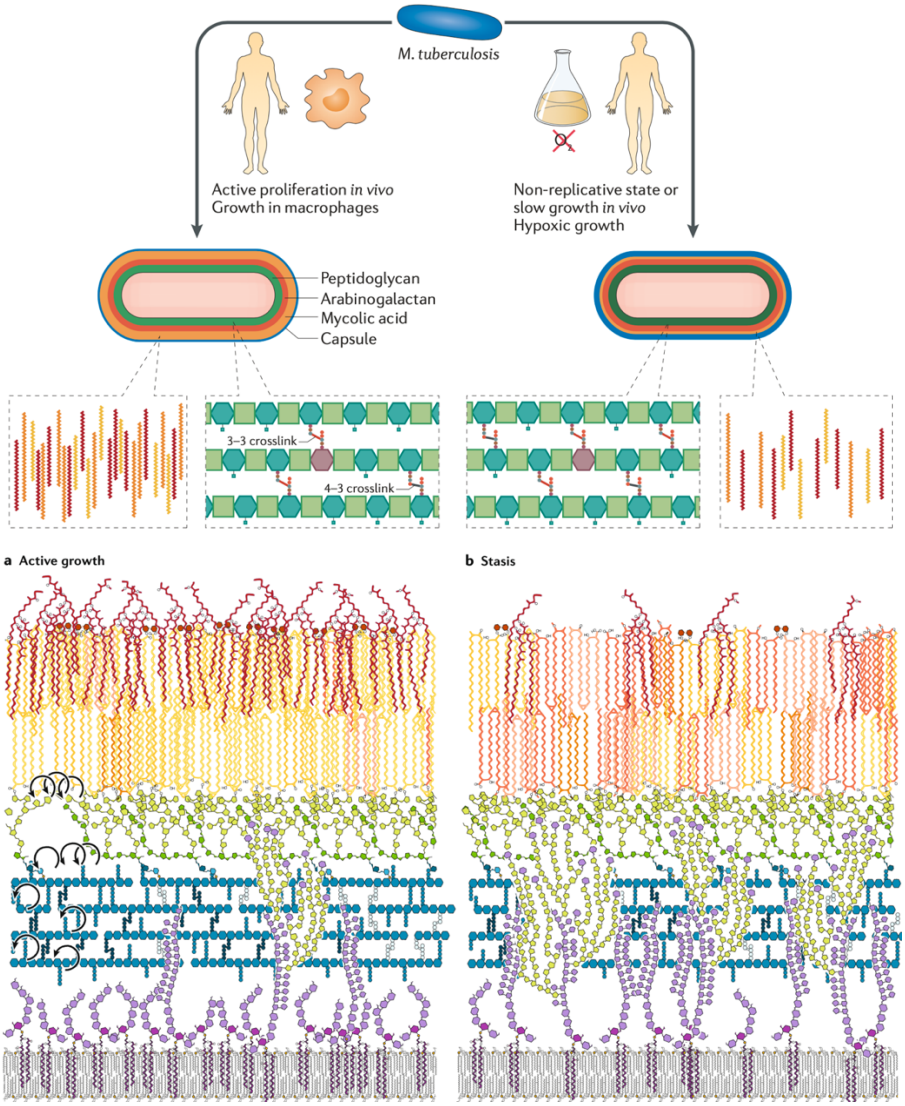

***Figure 9**. Structural differences of Mtb cell wall between an active growth form and stasis form, illustration issued from Dulberger et al.*[16,19]

Remodelling involves a radical change in the structure of the PG, the AG and the MA. As seen previously, the AG is a constitutive polysaccharide of the cell wall. So the carbohydrate backbone component of the AG is a rigid structure that requires the action of specific GHs able to hydrolyse polysaccharide chain in order to achieve remodelling of AG.[21]

I.5. Glycoside hydrolase

I.5.1. Generalities on glycosides hydrolases

Glycoside hydrolases (GH), commonly known as glycosidases, are very important enzymes and have various biological functions. Some have digestive functions and allow the degradation of oligo- and polysaccharides from our food into monomers essential to the metabolism.[22] Other glycosidases play an important immune role, for instance by their ability to hydrolyze the peptidoglycan of bacterial walls such as lysozyme.[23] Glycosidases are also involved in the post-translational modifications of proteins.[24] They belong to a class of enzymes that catalyze the cleavage of glycosidic bonds, by hydrolysis of the acetal, into an aglycone ROH and a hemiacetal, releasing a mono/polysaccharide (**Scheme 2**).[22]

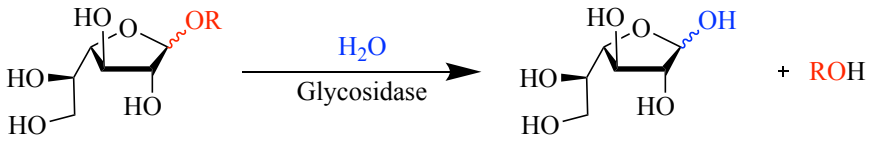

Scheme 2. *hydrolysis cleavage of polysaccharide catalysed by glycosidase*

Glycosidases have a very high recognition selectivity towards their substrate. This selectivity distinction is made on the basis of several criteria:

- The position in a polysaccharide chain: glycosidases can have an *endo* selectivity (if the hydrolysis takes place in the middle of a glycosidic chain, thus releasing a polysaccharide) or *exo* selectivity (if the hydrolysis is carried out on the terminal residue of a glycosidic chain, thus releasing a monosaccharide)
- The anomeric configuration of the substrate: α/β indicating the configuration of the asymmetric carbon carrying the acetal group. α-Glycosidase can only hydrolyze glycosides of configuration α.
- Saccharide type: Glycosidases show a high binding selectivity for the configuration of each asymmetric carbon of their substrates. Thus, galactosidases only cleave galactose residues.
- The ring size: furanose/pyranose indicating whether the substrate is respectively a 5- or 6-membered ring. Glycofuranosidases only hydrolyze glycosides in the furanose form (5-membered ring).
- The stereochemical outcome of the reaction: glycosidases are classified into two main classes according to the two possible mechanisms (inverting or retaining) depending on the configuration of the hemiacetal resulting from the hydrolysis

I.5.2. Mechanism

The studies conducted by Koshland in 1958 have highlighted two main mechanistic classes resulting in either an inversion or a retention of the anomeric carbon configuration.[25] The knowledge of this type of mechanism is important because it allows to determine which amino acids are involved in the hydrolysis of the substrate and to better understand how to envisage a strategy of inhibition of these GH.[24,26–28]

Those proceeding by inversion of configuration carry out the hydrolysis in a single step and the hemiacetal produced by the hydrolysis has an anomeric configuration opposite to that of the initial substrate. In this apparently concerted mechanism, two acidic residues play the roles of acid/base catalysis. The first one realizes the activation of the acetal by protonation exacerbating the electrophilic character of the acetal and ensuring the transfer of proton towards the leaving group. Then follows the nucleophilic attack of the water molecule on the opposite side of the acetal causing the inversion of the anomeric carbon configuration (**Scheme 3**).

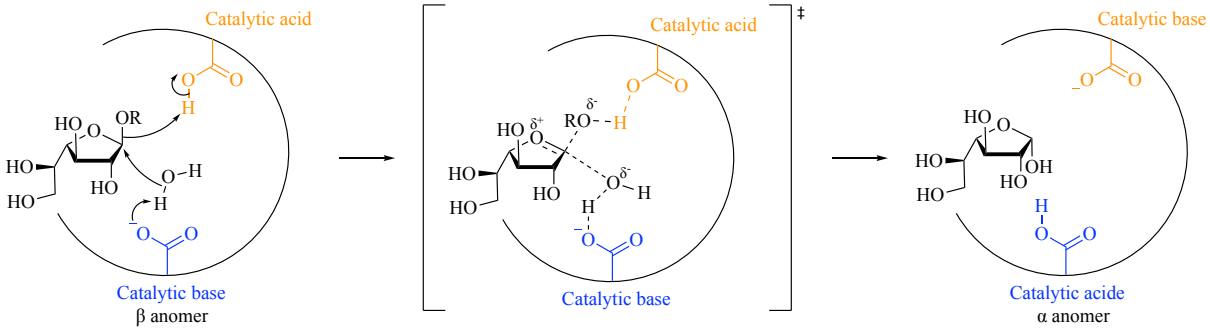

***Scheme 3**. inverting glycosidase mechanism*

Those proceeding by configuration retention carry out the hydrolysis in two steps, the hemiacetal produced by the hydrolysis has an anomeric configuration identical to that of the initial substrate. In this mechanism, an acidic residue acts as an acid catalyst allowing activation of the acetal by protonation exacerbating its electrophilic character and ensuring proton transfer to the leaving group. A second amino acid acts as a nucleophilic catalyst, the carboxylate attacks on the opposite side of the acetal causing the departure of the aglycone leaving group and a first inversion of the anomeric carbon configuration. This step also marks the establishment of a covalent bond between the glycosidase and its substrate. In a second step, the water molecule present in the catalytic pocket will hydrolyze this newly formed acetal causing the second inversion and the break of the covalent bond between the glycosidase and its substrate. This successive double inversion of configuration induces a conservation of the initial anomeric configuration (**Scheme 4**).

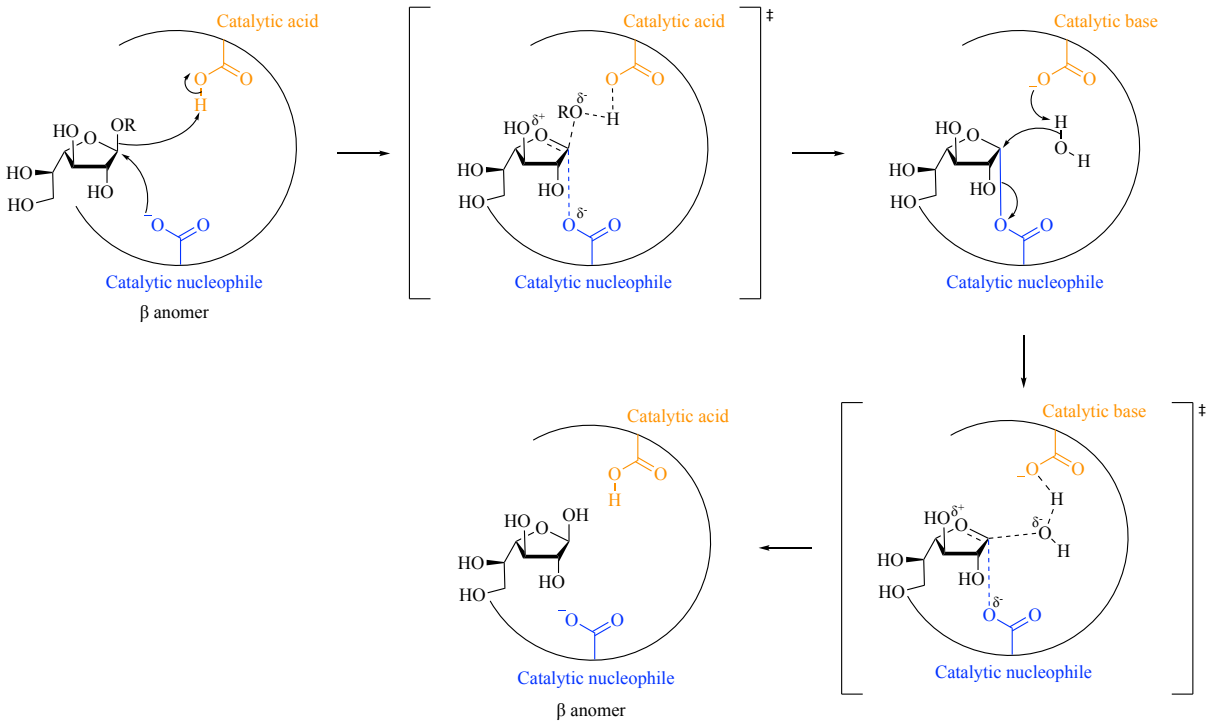

Scheme 4. *retaining glycosidase mechanism*

Regardless of whether they act by inversion or retention of anomeric configuration, glycosidases usually have two Asp/Glu residues in their catalytic pockets. In the first mechanism, these residues will act exclusively as acid/base catalysts residues whereas in the second case one of them will act as a nucleophilic catalyst, which is a striking difference in terms of inhibition design. Indeed, retaining glycosidases form a covalent enzyme-substrate intermediate. A GH of this type is then more interesting as it is possible, by preventing the second inversion, to inactivate it, i.e., to make it inoperative by irreversible covalent inhibition. This type of mechanism is therefore essential to achieve the inactivation of glycosidases. What distinguishes one amino acid acting as an acid/base catalyst from another acting as a nucleophilic catalyst is the spatial proximity they have with the substrate in the catalytic pocket. The study of crystallographic structures showed that the distance between the two catalytic Asp/Glu amino acids is not the same. It is about 5 Å for retaining GHs and it is in averages 9 Å for inverting GHs.[29]

I.6. Gl*f*H1, a novel glycosidase of *Mycobacterium tuberculosis*

A team of researchers from the University of Lille led by Professor Guérardel has discovered and characterized a new enzyme, Gl*f*H1, directly involved in the metabolism of cell wall galactan.[21] This enzyme seems to play a key role and gives to the bacteria this surprising structural property, the remodeling of galactan chain, constituting the intermediate layer of the mycobacterial cell wall. Its important role in these adaptations of the mycobacterial wall makes it a potential therapeutic target in the development of a future treatment.

Gl*f*H1 (Rv3096) is composed by 1140 coding base pairs for 379 amino acids. Its molecular weight was calculated at 40 382 Da (without signal peptide). The pH activity was studied between 3.0 to 9.0 with an optimum pH of enzymatic activity established to 4.5. Presence of Ca^{2+} showed a significant increase of enzymatic activity proving its important role for enzymatic activity. Kinetic constants were determined in presence of 0 – 5 mM of *p*NP- β -D-Gal*f*. K_m, k_{cat} and k_{cat} /K_m were established as 0.552 mM, 10.64 s^{-1} and 1.93 10^4 M^{-1} s^{-1} respectively.

Gl*f*H1 is an *exo*-β-retaining-galactofuranosyl hydrolase that participates in the remodeling by cleaving the β-galactofuranosyl residues of the galactan chain. It was shown that this GH had no activity for the β-galactopyranosyl form or the α-galactofuranosyl form demonstrating its substrate specificity for the furanose form and in the β configuration. Gl*f*H1 cleaves the terminal galactofuranosyl residue of the chain only, which proves its *exo*-selectivity. Then, after characterization of the hydrolysis product galactoside, it was found to be predominantly of anomeric β configuration, demonstrating that Gl*f*H1 employs an anomeric stereochemical retention mechanism. Amino acids involved are Glu-170 and Glu-268, as general acid/base residue and nuclophilic residue respectively. This type of mechanism makes Gl*f*H1 of great interest as it can be inactivated by covalent inhibition using a glycomimetic able to mimic the cationic transition state of a β galactosfuranosyde hydrolysis.

I.7. Inhibition strategy

To participate in the cleavage of the D-Gal*f* residues of AG, this new glycosidase acts by a mechanism of retaining of configuration. This mechanism, passing through a covalent enzyme-substrate intermediate, potentially allows an irreversible covalent inhibition between the enzyme and a properly designed inhibitor. This characteristic makes Gl*f*H1 a target of choice for inactivation.[30] A way to design high-affinity inhibitors is to mimic the transition state. First, the transition state has likely a strong cationic character at the anomeric carbon and a sp^2 character. The strategy is to find a glycomimetic analogue of the substrate with these two characteristics, able to mimic its transition state while increasing the activation energy of the hydrolysis reaction.[26,28] The increase in activation energy of the second step is able to prevent the second inversion and hydrolysis of the covalent enzyme-substrate complex from taking place. The enzyme becomes inoperative. This difference makes them prime targets for inactivation, proving to be an asset in drug design.

Many methods, illustrated in **Figure 10**, for the inactivation of retaining GH exist and could be potentially envisioned for inactivation of Gl*f*H1.[31] Fluorinated molecules (**Figure 10b)** act by destabilizing the transition state, the inductive electron-withdrawing effect of the fluorine atom destabilizes the oxycarbenium character of the transition state decreasing the rate of hydrolysis of the covalent complex.[32] Substrate analogues bearing an epoxide, shown in **Figure 10c**, are irreversible inhibitors by preventing the hydrolysis of the covalent enzyme-inhibitor bond. The nucleophilic catalysis embodied by the Asp/Glu amino acid residue attacks and opens the electrophilic epoxide. The opening of the epoxide generates an alcohol and the non-hydrolysable covalent bond. Indeed, this one is an ester, much less electrophilic and reactive than the acetal of the natural substrate. The latter then remains bound to the enzyme and renders it inoperative.[33,34] Haloketones glycosides are another type of electrophilic inactivating molecules (**Figure 10d**) that employ an electrophilic trap which irreversibly alkylate nucleophilic residues in the catalytic pocket. Photoactive glycosides (**Figure 10e)** use diazirines as precursors of carbene upon photoexcitation which react, upon photoexcitation, with neighboring residues to form covalent link. Finally, quinone methyl glycosides (**Figure 10f**) are molecules that released, after enzymatic hydrolysis, a reactive molecule able to alkylate nucleophilic residues.[33]

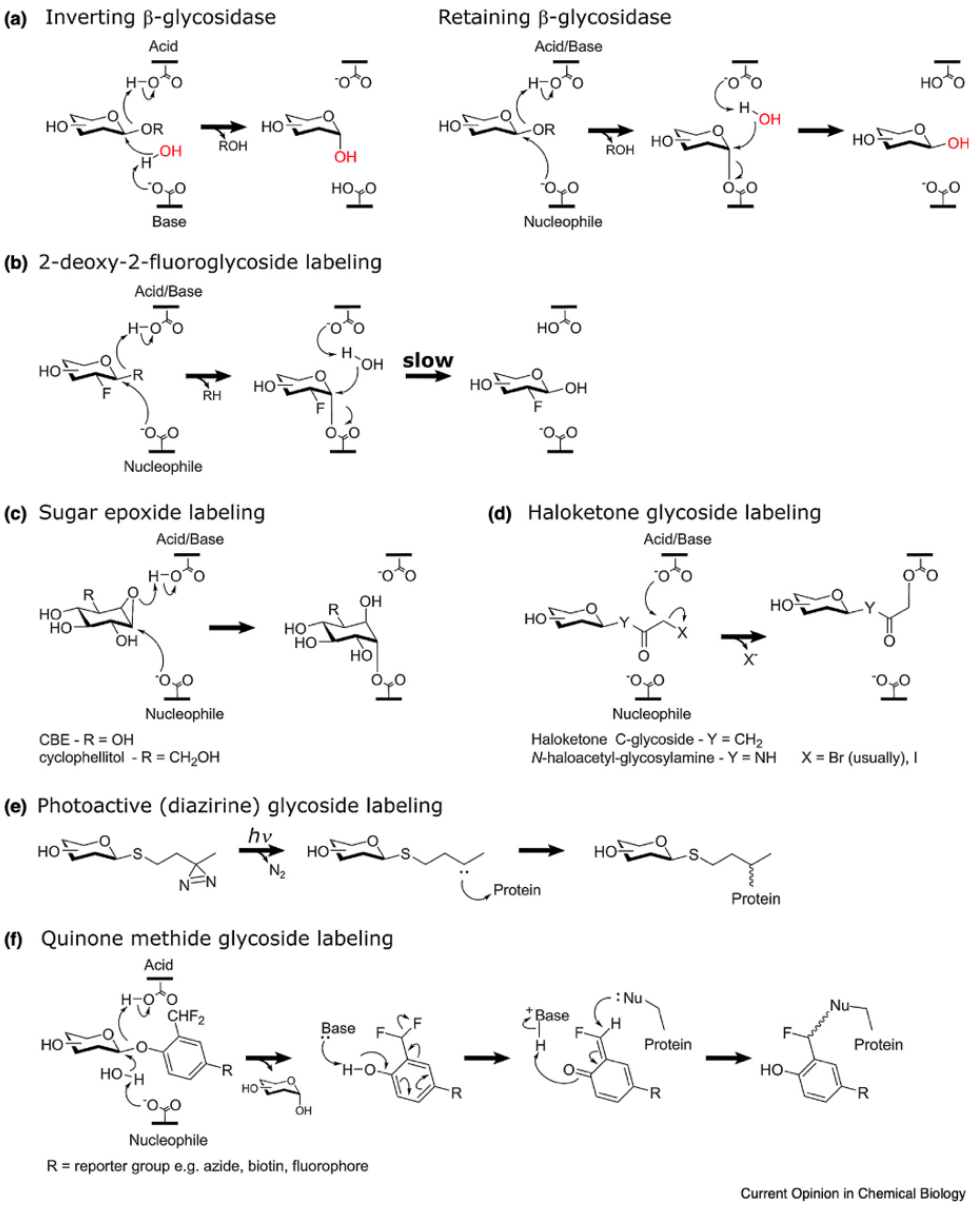

***Figure 10**. mechanism of glycosides hydrolase and inhibitor strategy, illustration taken from Wu L. et al.*[33]

Similarly, to epoxide, it has been shown that aziridine glycoside analogues can also be potential inactivating molecules. Many GHs inhibitors incorporate a basic nitrogen atom because, when protonated, it mimics the incipient charge of the cationic transition state. The cationic character may also increase the affinity for the catalytic pocket. Indeed, GHs stabilize the positive charge generated by the oxycarbenium intermediate. The positive charge of the aziridinium ion can further mimic this cationic character and make the affinity of the inhibitor for the enzyme even more favorable. With a pKa close to 8 for the aziridinium/aziridine acid-base couple, this protonation can, at least partially, take place in physiological media or in a catalytic pocket. An advantage of the use of aziridine compared to an epoxide is that it is trivalent, it is therefore possible to substitute the hydrogen and to insert an R group used as a reporter to carry out, for

example, kinetic tests or labelling studies. The team of Professor Overkleeft has developed multiple approaches to design GH inhibitors with aziridine groups. Among them, many conduritol derivatives have demonstrated their ability to inactivate glycosidases.[35] This is the case of cyclophellitol aziridine (**12**, **Figure 11**), and 1,6-epi-cyclophellitol aziridine **13** which have been shown to be potent covalent inhibitors of human retaining glucosylceramidases.[36]

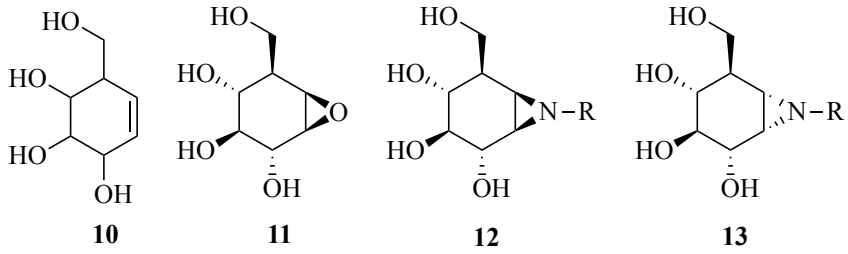

Figure 11**. structure of conduritol **10**, cyclophellitol 7, cyclophellitol aziridine **8** and 1,6-Epi-cyclophellitol aziridine **9

Different approaches were developed to synthesize aziridines from conduritol derivatives. The first approach, described by Kallemeijn *et al*., [37] allows to obtain cyclophellitol aziridine **16** from conduritol **14** in four steps as described in **Scheme 5**.

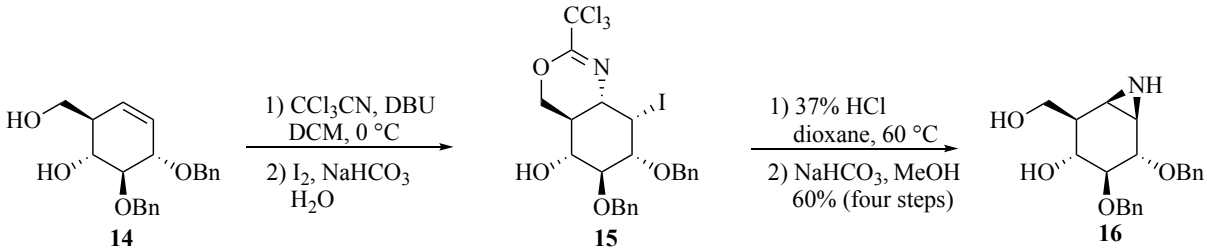

***Scheme 5.** formation of cyclophellitol aziridine issued from Kallemeijn et al.*[37]

A second approach used by Willems *et al*.[38] employ an intermediate epoxide (**Scheme 6**). This reaction is done in three steps with an overall yield of 12%. The first step is the epoxidation of conduritol **17** to give epoxide **18** followed by the opening of the epoxide by an azide and finally the reduction of this azide to give the conduritol aziridine **19**.

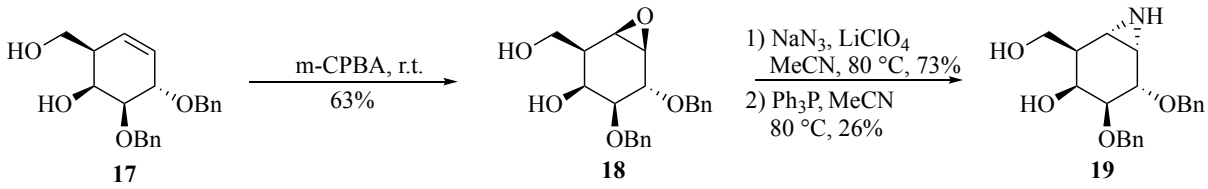

***Scheme 6**. formation of a conduritol aziridine using an epoxyde intermediate (18)*

Another approach described by Schröder *et al*.[39] consists in a one-step reaction at room temperature using dinitrophenylhydroxylamine (DPH) in the presence of a rhodium catalyst in trifluoroethanol to give exclusively aziridine **21b** as shown in **Scheme 7**.

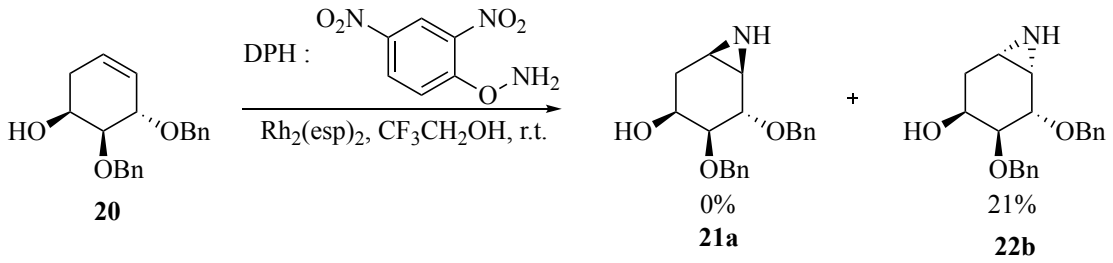

Scheme 7. *aziridination reaction on cyclohexene precursor (**20**) using DPH*

The last method, described by Artola *et al.*,[40] allows to directly obtain an aziridine from the alkene by using aminoquinazolines (R^1-Q-NH_2 où R^1: CF_3, Et, OH). Deprotection of aziridine **24** can then be performed under Birch conditions to give aziridine **25** (**scheme 8**).

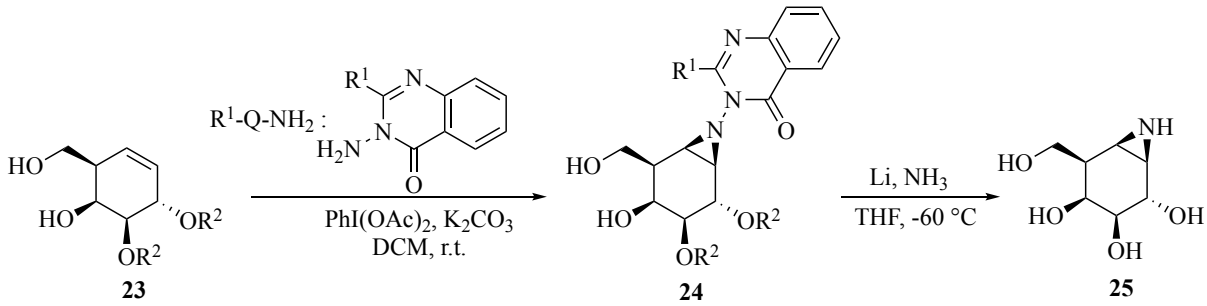

Scheme 8*. aziridination reaction on conduritol (**23**) using a hydroxylamine quinazoline to afford conduritol aziridine (**25**).*

II. OBJECTIVES

Studies conducted by Professor Guérardel and his team on Gl*f*H1 are mainly based on molecular biology and biochemical investigations.[21] It is crucial to develop a method to achieve an irreversible covalent inhibition of this glycosidase in order to deepen the knowledge of this glycosidase. In addition to obtaining the result of kinetic parameters, inactivation can provide more information about the active site and improve structural knowledge by X-ray crystallographic studies on covalent enzyme-inactivator adduct.

Based on the different strategies of inhibition of inverting GHs, fluorinated probe **26** in **Figure 12**, in our laboratory and displayed a characteristic time-dependent inactivation profile capable of having an inhibitory activity have been synthesized previously.

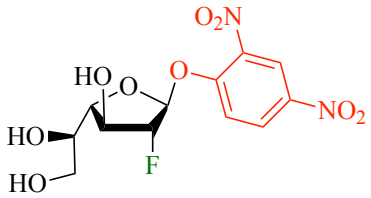

26

***Figure 12**. fluorinated probe*

As seen above, other inactivator design strategies exist, in particular, carbasugars bearing an aziridine moiety. The mechanism of inactivation by carbasugar aziridines, illustrated in **Scheme 9**, is quite similar to that of the epoxide with a few differences. The aziridine, once protonated, becomes a more electrophilic aziridinium ion than the epoxide thus increasing, the rate of the nucleophilic attack. The tension of the three-membered ring makes the *pseudo*anomeric carbon more reactive. After the aziridine, the covalent bond the inactivator and the enzyme are covalently linked by an ester bond. The pseudo anomeric carbon is therefore no longer electrophilic enough to be hydrolyzed. [34]

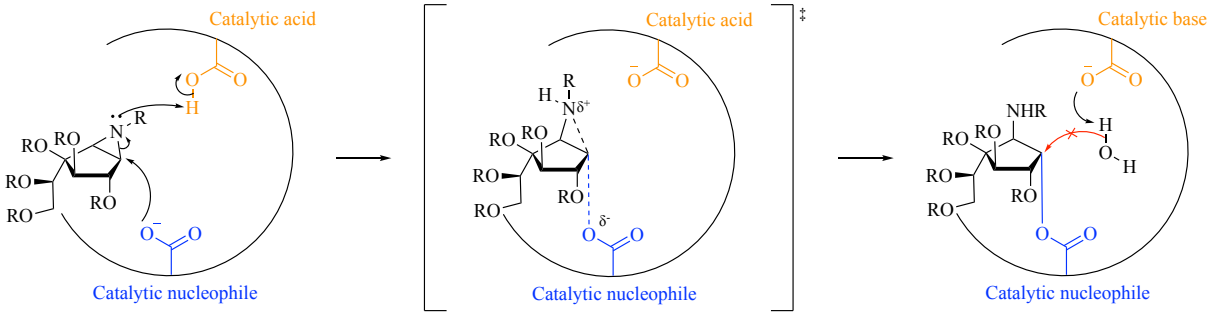

***Scheme 9**. possible covalent inhibition mechanism of a retaining galactosidase by a glycomimetic bearing an aziridine moiety*

It just legitimate to consider a new molecule potentially capable of inactivating Glf*H*1 based on aziridine properties. This molecule must be an analogue of a galactofuranosyl residue mimicking the natural substrate **27** in **Figure 13**, carrying an aziridine group mimicking the cationic character of the transition state of the natural substrate **28** and preventing hydrolysis of the covalent enzyme-substrate complex. The objective is to synthesize a molecule gathering all these characteristics to become a potential inactivator **29** of Glf*H*1.

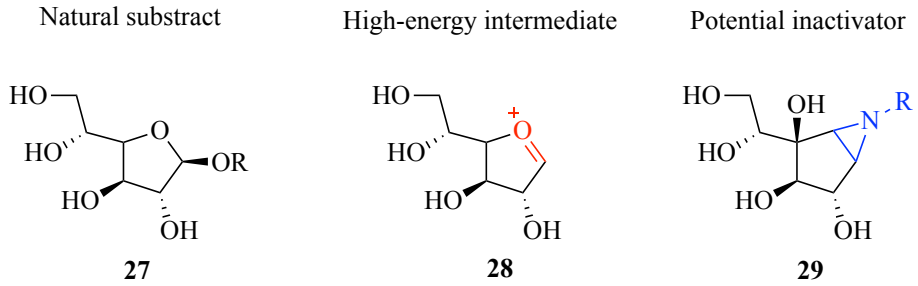

Figure 13**. structures of the natural substract **28**, high-energy intermediate **29** and potential inactivator of GlfH1 **30

In the next chapter, we will detail our retrosynthetic analysis of molecule **29** and will describe our synthetic efforts towards this achievement.

III. RESULTS

III.1. Synthetic pathway

The desired aziridine **30** can be obtained directly from the cyclopentene precursor **31** via various methods explained later (**Scheme 10**).

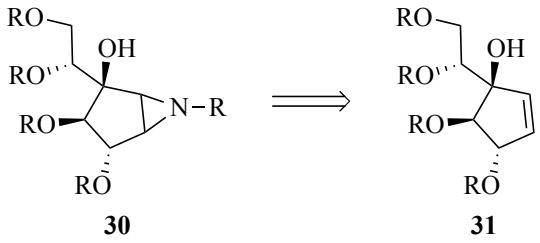

Scheme 10. *Alkene **31** as precursor of aziridine **30**.*

This cyclopentene precursor **31** can be obtained via multi-step synthesis from D-galactose. D-galactose has the advantage of being commercially available and cheap while having the desired configurations of the asymmetric centers of the carbons at C-2, C-3, C-4 and C-5 positions.

The retrosynthetic strategy, detailed in **Scheme 11**, to obtain the cyclopentene precursor **31** is based on the work of former CBO PhD student who completed the synthesis of 6-membered ring cycloalkenes.[41–43] Our strategy consists in performing a ring-closing metathesis of diene **32** The latter can be obtained by a double olefination. An insertion of a first olefin can be realized by an addition of a vinylmagnesium bromide on the ketone intermediate **33** and the second olefin by a Wittig olefination reaction on a hemiacetal resulting from the reduction of lactone **34**. Finally, this lactone can be generated by an oxidation of commercially available D-galactose **35**.

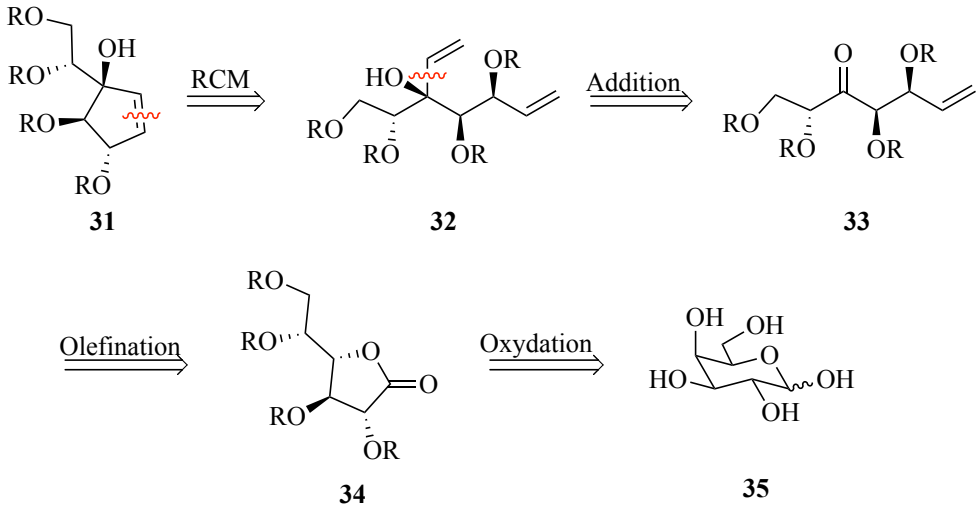

Scheme 11*. Retrosynthesis of cyclopentene **31** (R are protecting groups)*

III.2. Formation of lactones **43**, **36** and **37**

To obtain the protected lactone **36**, the first step is to oxidize D-galactose using bromine. This method is widely used to make sugar lactones and usefull to avoid other methods using microwaves, difficult to implement for a large-scale reaction. This reaction was performed under the same conditions as those described and optimized by El Bkassiny *et al.* [43, 44] in presence of bromine (1.05 equiv.) and barium carbonate (2.2 equiv.) in water for six hours (**Scheme 12**).

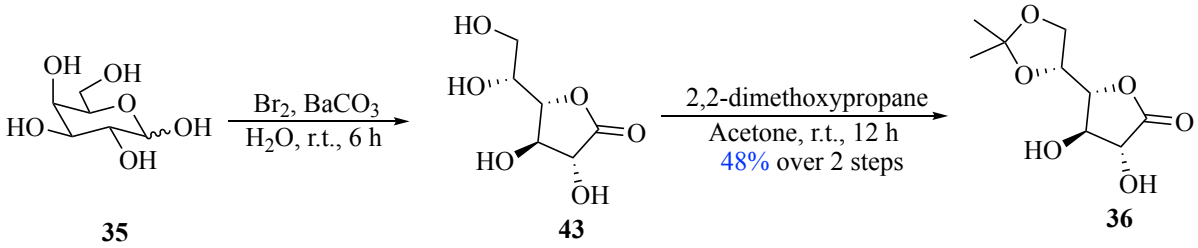

***Scheme 12**. oxydation of D-galactose **35** to make 1,4-galactono-lactone **36**.*

Although carbohydrates thermodynamically favour pyranoses when hemiacetals are in equilibrium, 1,4-lactone **36** is the only oxidation product formed under these conditions as shown in **Scheme 12**.[45] This oxidation is therefore an effective way to lock the carbohydrate into the desired 5-membered ring **43**.[46] However, it is necessary to protect the C-5 alcohol so that it cannot generate a pyranose during the following steps. Therefore, an acetonide was planned in the synthesis scheme. This acetonide formation is highly regioselective for the protection of exocyclic alcohols. Indeed, the formation of acetals with the other alcohols on either side are less favoured. Immediately after oxidation, protection of the diol was performed with p-toluenesulfonic acid in acetone in the presence of 2,2-dimethoxypropane, to avoid formation of water and to shift the equilibrium toward acetal formation **36**. This stepwise reaction could be achieved in 48% yield for two steps.

Once the furanose configuration is locked, the next step is to protect the other two alcohols by placing benzyl ethers as protecting groups (**Scheme 13**).

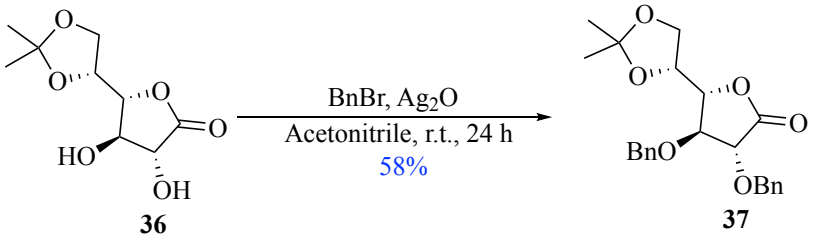

***Scheme 13**. benzylation of cyclic alcohols*

This benzylation reaction was performed under basic conditions in the presence of benzyl bromide (11 equiv.) and silver (I) oxide (4 equiv.) in acetonitrile for 24 hours. In contrast to a classical benzylation reaction performed with sodium hydride, the use of silver oxide as a base allows milder conditions and prevents the lactone degradation. However, the reaction remains problematic in two aspects and optimization is illustrated in **Table 1**.

The first is a conversion problem despite the use of a large excess of benzyl bromide, it was not possible to obtain the fully benzylated product in good yield. Similarly, time does not appear to have a positive influence on yield and conversion as shown for entry 3 and 4 in **Table 1**. Indeed, the reaction has been tested over several time intervals between 24 and 36 hours without significant differences. The quality of the silver (I) oxide also seems to have an effect on the conversion and yield. In general, reactions using commercial grade silver (I) oxide showed better conversion and yields and reduced the formation of unwanted side products compared to synthetic silver (I) oxide as shown with entry 6 and 7 compared to 3 and 5 in **Table 1**. Synthetic silver (I) oxide was made by mixing silver nitrate with sodium hydroxide to afford silver (I) oxide as an insoluble black solid. This black solid was filtrated, washed with EtOH and dried under vacuum to afford a black powder.

The second problematic aspect is the procedure performed to isolate the final product. This protocol, developed by former researchers of the laboratory, was, after filtration of silver oxide (I) on celite, to precipitate the product by adding cold pentane. The product precipitates and forms a white powder recoverable by filtration. However, this method did not allow to totally recover the product and generated variable yields ranging from 13 to 95%. Yield of 95% shown in entry 2 in **Table 1** seems the best condition but was not reproducible. Instead of trying to filter the product, it was considered to evaporate the remaining large amount of benzyl bromide but without success due to its high boiling temperature. The solution that has worked best so far is a purification by chromatographic column using a slow eluent (Cy/EtOAc 99:01 → 80:20). While failing to achieve good conversion, this purification technique still provided more reproducible yields unlike those related to product precipitation as shown in entry 5 and 7 in **Table 1**. Other experimental parameters such as temperature or the choice of another solvent could also have been studied in order to improve the yield of this reaction.

Table 1**. conditions of benzylation of lactone **36

Entry	Scale mass (g)	Equivalent BnBr:Ag_2O	Ag_2O Quality	Time (h)	Purification	Yield
1	1.000	3:3	synthetic	24	Precipitation	0%
2	0.100	11:4	synthetic	24	Precipitation	95%
3	2.500	11:4	synthetic	24	Precipitation	13%
4	8.000	11:4	synthetic	36	Precipitation	14%
5	0.600	11:4	synthetic	24	Chromato.	20%
6	2.200	11:4	commercial	24	Precipitation	48%
7	8.000	11:4	commercial	24	Chromato.	58%

Another possible solution would be to use other protective groups. However, the optimization of benzylation was realized in parallel of the development of the next steps. Therefore, the use of other protecting groups was not considered. Then, once substrate **37** was fully protected, we could continue the synthesis to introduce the two olefines.

III.3. Introduction of the first olefin

The first olefin is generated by a Wittig olefination. To prepare the substrate to perform the olefination, it is necessary to reduce the lactone **37** to lactol **38**. This reaction was performed using two reducing agents to compare their efficiency: diisobutylaluminum hydride (DIBAL-H) and lithium tri-sec-butylborohydride also known as L-Selectride® as shown in **Scheme 14**.

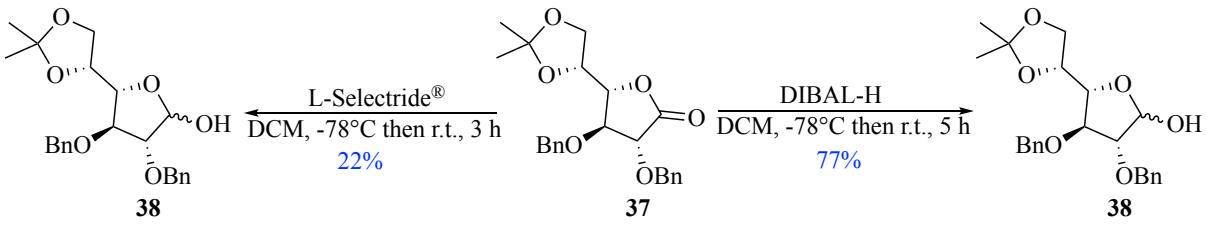

Scheme 14.** reduction of lactone **37** into lactol **38

The first reaction performed with diisobutylaluminum hydride (1.25 equiv.) in dichloromethane at room temperature for five hours, Providing lactone **38** in 77%. The reaction using L-Selectride® as reducing agent was carried out, following the procedure reported by Yin B. *et al.*,[47] in the presence of L-Selectride® (1.5 equiv.) in dichloromethane at room temperature for three hours. The reaction reached an isolated yield of 22%. DIBAL-H was thus a better reducing agent to reduce the lactone **37**.

Lactol **38** is a suitable precursor to perform the Wittig olefination as it is a masked aldehyde. Indeed, the hemiacetal **38** is in equilibrium with its linear aldehyde form **38'**. It is this acyclic form carrying the aldehyde function which is active to carry out the Wittig reaction (**Scheme 15**).

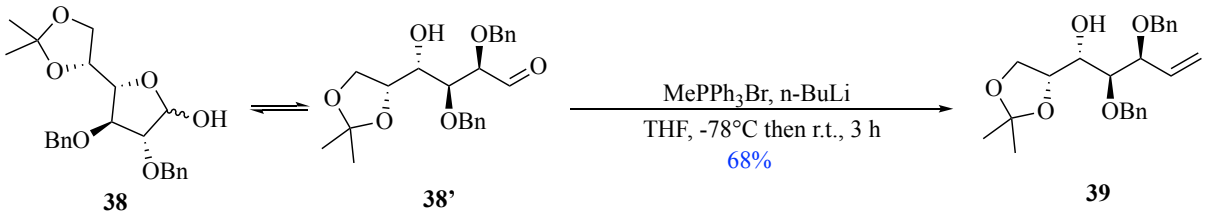

38 **38'** **39**

Scheme 15**. Wittig olefination of lactol **38

Prior to the initiation of the reaction, lactol **38** is pre-treated with one equivalent of n-butyllithium (n-BuLi) to deprotonate the lactol. Once deprotonated, the substrate is mixed with phosphonium ylide to give the olefin **39** that was purified by silica gel chromatography in an isolated yield of up to 68%.

III.4. Installation of the second olefin

The strategy to form the second olefin consists in performing an addition of an vinyl Grignard on an intermediate ketone **40**, obtained by an oxidation **39** of the alcohol as shown in **Scheme 16.**

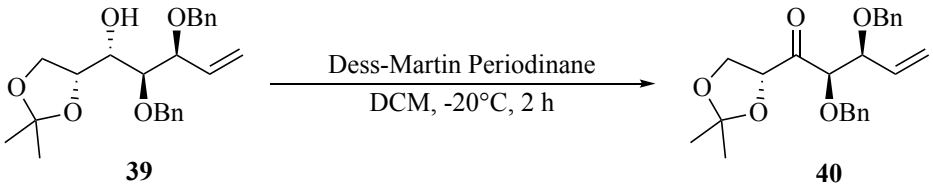

39 **40**

***Scheme 16**. oxydation of alcohol **39** to afford intermediate cetone **40**.*

This alcohol oxidation is performed with Dess-Martin periodinane **45**, (structure in **Figure 14**) as the oxidizing agent in dichloromethane at -20 °C for two hours. The use of this oxidizing agent has many advantages: the reaction is milder than a Swern oxidation and proceeds rapidly with high yields and simplified procedures. This reagent, composed of a stabilized hypervalent iodine as an electron collector, is very useful for the oxidation of primary and secondary alcohols to aldehydes and ketones at room temperature.[48] The resulting crude reaction mixture being pure (after work-up), the following reaction was performed directly without chromatography.

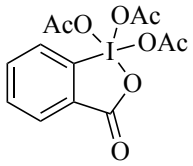

Dess-Martin Periodinane

45

***Figure 14**. structure of Dess-Martin Periodinane*

Once the intermediate ketone **40** generated, the Grignard reaction with vinylmagnesium bromide in tetrahydrofuran (THF) took place for three hours at -20 °C (**Scheme 17**).

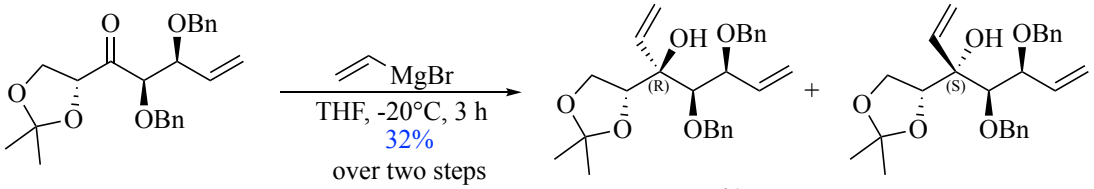

40 **R-41** **S-41**

***Scheme 17**. Grignard addition on cetone (**40**)*

The reaction leads to the formation of two diastereomers: **R-41** and **S-41**, in proportion 9:1 (assessed by ^{1}H NMR). Due to the conformational freedom associated with the acyclic form, it was not yet possible to determine the absolute configuration of the predominant stereoisomer. The two diastereomers could be separated by chromatography. The overall isolated yield of the oxidation and Grignard addition for the pure diastereomer is 32% over two steps. With the diene in hand, the cyclization could be considered.

III.5. Synthesis of cyclopentene precursor using ring closure metathesis (RCM)

Ring closure metathesis (RCM) is a type of metathesis that condenses two intramolecular terminal olefins to give a cycloalkene.[49] This transformation is entropically favorable by the release of a volatile ethylene molecule, a real driving force to shift the equilibrium towards the desired cycloalkene form. However, this driving force can also be favorable to the acyclic dienes metathesis polymerisation (ADMET) polymerization process. There is thus a competition between these two reactions which are the RCM and ADMET as shown in **Scheme 18**. It is thus advisable to work under conditions of high dilution to minimize the intermolecular reactions and thus the oligomerization. At high dilution, the probability of meeting between

two molecules becomes negligible and it is the intramolecular reaction, the RCM, which is privileged. [50]

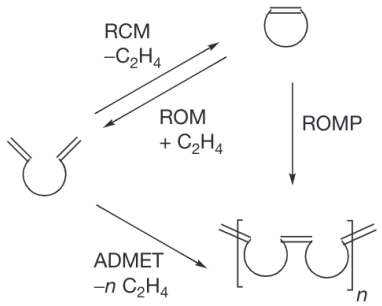

Scheme 18. *different types of olefin metathesis. Illustration issued from Zukowska K.* [49]

The use of a suitable catalyst is essential to carry out this RCM. Today, about a hundred metathesis catalysts have been developed. The first one centered on molybdenum (**Mol-I**) (**Figure 15**) was invented by Schrock. Some of them proved to be effective but were sensitive to air and humidity, which considerably reduced their range of applications. A new generation of metathesis catalysts based on ruthenium (**Figure 15**), much more stable in air and less sensitive to humidity, was then developed by Grubbs. Many such catalysts exist with different ligands such as phosphines, *N*-heterocyclic carbenes and oxides.

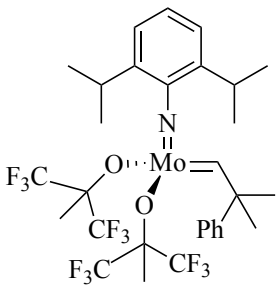

Mol-I

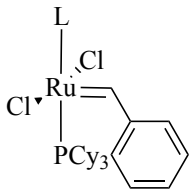

Gru I

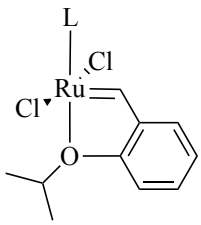

Hov-G I

L = PCy_3 **Gru I** **Hov-G I**

L = SIMes **Gru II** **Hov-G II**

L = SIPr **Gru SIPr** **Hov-G SIPr**

PCy_3 = 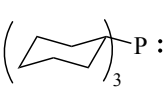

SIMes = 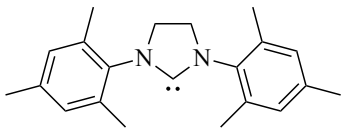

SIPr = 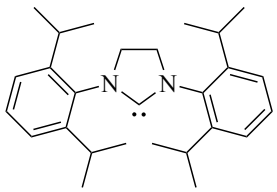

Figure 15*. main commercial catalysts for olefin metathesis*

Hoveyda-Grubbs (**Hov-G**) type catalysts are shown to be better RCM initiators than Ruthenium complexes possessing a phosphine ligand (**Gru**). It has also been shown that $P(Cy)_3$ phosphine ligands are generally slower than ruthenium complexes without phosphine. This is mainly due

to the electron density provided by the oxygen atom which makes ruthenium more reactive.[46] Moreover, the second generation Hoveyda-Grubbs type catalyst (**Hov-G II**) has already demonstrated its efficiency with conditions already optimized in the synthesis strategy developed by Bkassiny *et al.*, in our laboratory, which further supports the use of this catalyst to perform this metathesis.[42]

From the diene **41**, the ring closure metathesis (RCM) could be performed to obtain the cyclopentene. This reaction was performed with Hoveyda-Grubbs (II) catalyst in toluene at 80 °C for two hours (**Scheme 19**).

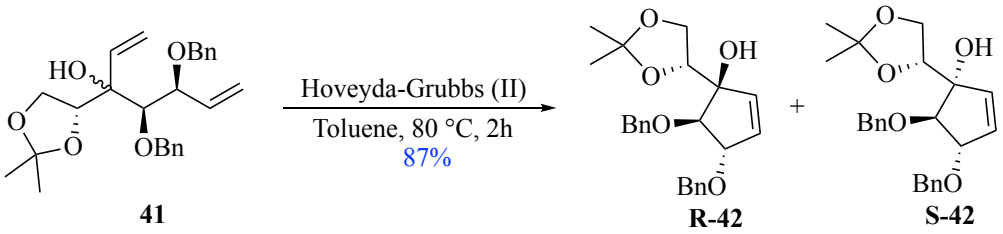

41 **R-42** **S-42**

***Scheme 19**. formation of cyclopentene by ring closing metathesis*

After only two hours, TLC already showed an almost complete conversion of the starting material. After purification of the reaction crude on silica gel column (Cy/EtOAc 80:20), the isolated product **42** was obtained in up to 87% yield on a 150 mg scale.

At this stage, once the metathesis was performed, it ws now possible to determine the configuration of the C-4 carbon. nOe experiments, realized by L.Chêne, was led by irradiation of H-2. As a result, no correlation between H-2 and H-5 was observed. This observation supports the hypothesis that the desired **R-42** was the major product.

III.6. Formation of aziridine

The approach considered to achieve aziridination is the one described by Qadir T. *et al*. (**Figure 16 A**)[51] . This method employs chloramine-T **48** whose structure is detailed in **Figure 16 B**. Chloramine-T is a very classical reagent for the formation of aziridines for several reasons. First, chloramine-T is cheap and allows a quick reaction even at room temperature. [52]

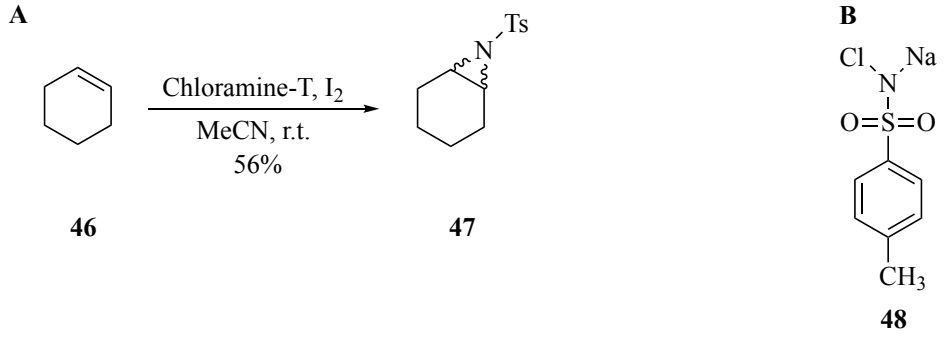

Figure 16. A. Aziridination reaction using chloramine-T performed on cyclohexene 46. B. Structure of Chloramine-T 47.

The latter method was first considered in order to achieve the objective of forming an aziridine because of its availability and ease of implementation. The procedure followed was developed by Mordini *et al*. and was performed with chloramine-T (1.5 equiv.) in the presence of iodine (0.4 equiv.) in acetonitrile at room temperature (**Scheme 20**). [52]

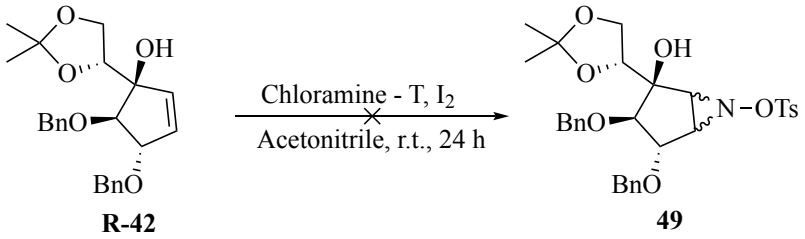

Scheme 20. aziridination reaction on cyclopentene precursor 42 using chloramine-T and iodine

First, chloramine-T is mixed with iodine for thirty minutes, then the alkene is added and the reaction is left for 24 h. After 24 h, the TLC control seems to show the absence of conversion of the reaction. From the crude NMR, it turned out that the reaction did not take place, as the cyclopentene precursor did not react. It is also interesting to note that there was no halogenation reaction with iodine on the alkene either. The hypothesis put forward here is that cyclopentene has a very low nucleophilicity due to its important steric hindrance generated by the immediate proximity of the protective groups. To support this hypothesis, the halogenation reaction with diiodine on the cyclopentene precursor was tested, with iodine playing the role of a very electrophilic species. The reaction was carried out over three hours in acetonitrile at room temperature with an excess of iodine (1.5 equiv.) without success. This hypothesis may also

explain why the epoxidation reaction, tested by L. Chêne, on the cyclopentene precursor in the presence of m-CPBA did not occur.

In conclusion, it is potentially unlikely to perform this aziridination based on the nucleophilic properties of this cyclopentene. This one having a too weak nucleophilicity because of its consequent steric hindrance. It would therefore be more appropriate to consider an aziridination of this alkene via other methods involving nitrenes or nitrene analogues.

IV. CONCLUSIONS

The objectives of this master thesis were first to form a potential inactivator of Glf*H*1, a carbasugar bearing an aziridine moiety capable of mimicking the transition state of the natural substrate galactofuranose. This aziridine **30** can be formed from a cyclopentene precursor **31**. The latter can be synthesized from D-galactose as starting material (**Scheme 21**).

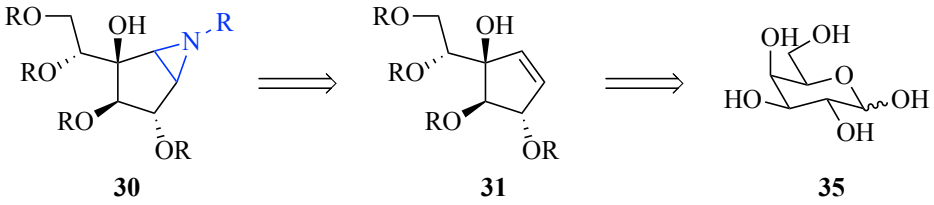

30 **31** **35**

***Scheme 21**. retrosynthetic approach of formation of aziridine **30** as potential inactivator of GlfH1*

The first goal to form the cyclopentene precursor **31** could be successfully achieved. The synthetic approach, shown in **Scheme 22**, was first to convert the six-membered ring of D-galactose to a five-membered ring **37** with the installation of intermediate protecting groups. In contrast to the acetonide formation, the subsequent benzylation proved troublesome. An improvement of the yield and a better reproducibility of the results could be obtained thanks to the studies on the impact of the quality of the silver (I) oxide and of the purification method on this reaction. Then, the first olefin was installed with a Wittig reaction on a hemiacetal **38** playing the role of masked aldehyde to obtain **39**. Then, the second olefin was generated by means of an intermediate ketone **40** obtained by an oxidation using Dess-Martin periodinane. The addition of a vinyl Grignard on this intermediate ketone was efficient and highly diastereoselective in favor of the desired diastereoisomer. Finally, an RCM can take place to cyclize these two olefins and form the expected protected cyclopentene **42**. This cyclopentene **42** was obtained with an overall yield of 4% over eight steps.

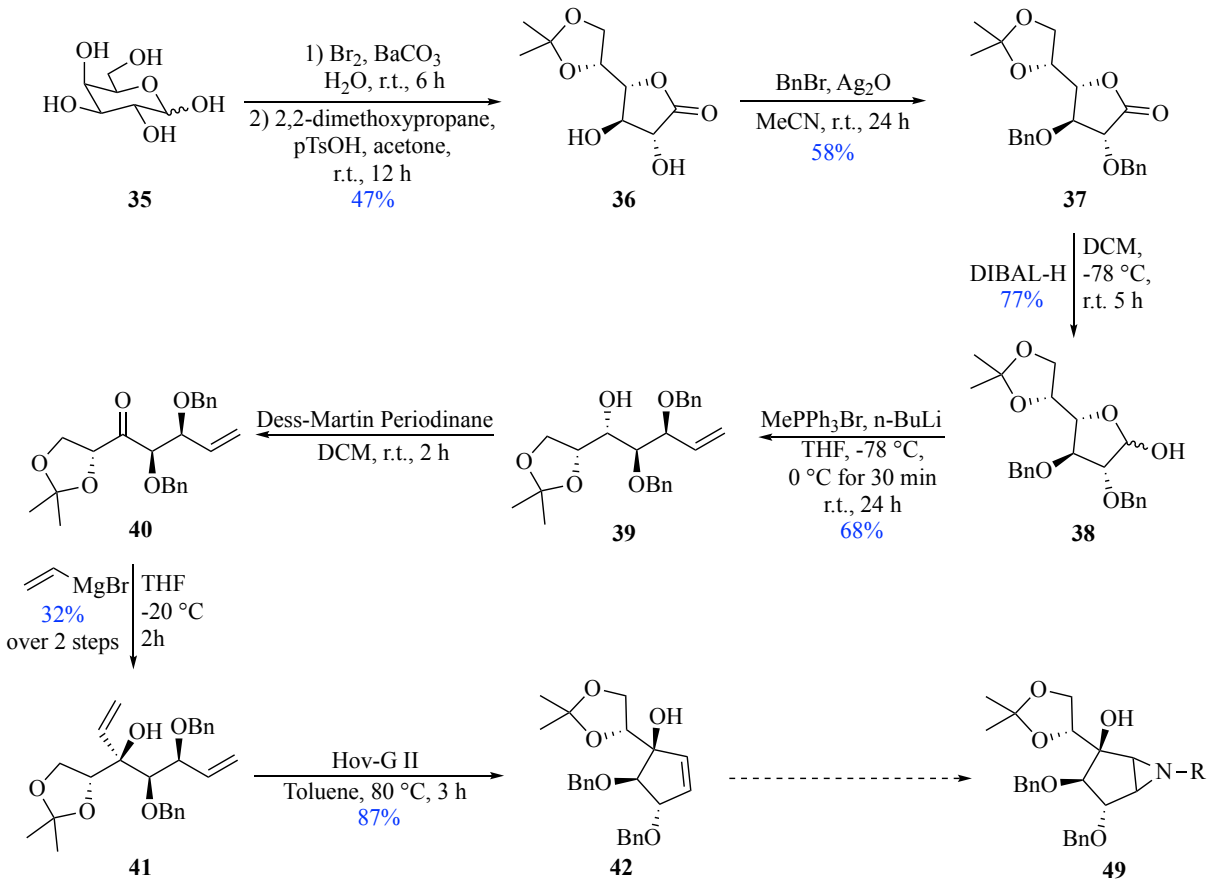

***Scheme 22**. result of complete synthesis of cyclopentene precursor (42)*

Once the first objective of synthesizing the cyclopentene precursor was achieved, it could then be used as a starting material to form an aziridine. The envisaged aziridination involved the use of chloramine-T in the presence of iodine. After 24 h, it was found that no reaction on cyclopentene took place, neither with chloramine-T nor with iodine. The nucleophilic character of this cyclic alkene is thus questioned.

V. OUTLOOKS

V.1. Synthesis of aziridines

An interesting outlook is to investigate other methods to synthesize aziridines from a cyclopentene precursor. With the identification of a very weakly nucleophilic alkene, methods based on the nucleophilicity of the cyclopentene precursor or using epoxide intermediate should be avoid. Other methods based on nitrenes or nitrene analogues must be considered for the aziridination of the cyclopentene precursor **R-42**. The methods described by Schröder *et al*. (pathway **A** in **Scheme 23**) and by Artola *et al*. (pathway **B** in **Scheme 23**) seem to be good alternatives for performing the aziridination reaction.

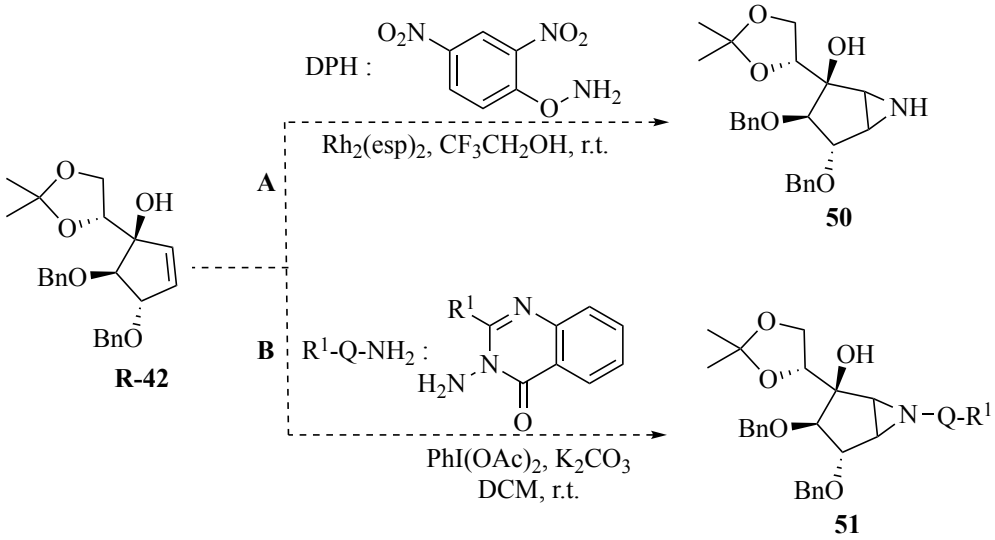

Scheme 23. *Hypothetic pathways to synthesize aziridines*

In pathway **A**, the Rh catalyst seem to coordinate with amino group in DPH. A Rh-nitrene is formed with release of dinitrophenol to afford aziridine **50**. In pathway **B**, a hydrazine plays the role of aziridinating agent (R^1-Q-NH_2). Atkinson *et al.* concluded that *N*-acetoxy-aminoquinazolone (R^1-Q-NHOAc) is the reactive intermediate.[54] This method could work on poorly nucleophilic cycloalkenes. Interestingly, the deprotection of **51** (under Birch conditions) might be realized, under the same reducing conditions as those required for the deprotection of benzyl ethers, which could be advantageous.

V.2. Planned biological studies

In the future, once the aziridination has been successfully performed, it will be possible to carry out biological tests on this new aziridine. First, inhibition against Gl*f*H1 will be tested in order to demonstrate whether it is capable of having an inactivating activity on Gl*f*H1 and to determine the kinetic parameters of inhibition. The first interesting parameter to study is the inhibition binding constant (K_i) which represents the dissociation constant of the non-covalent enzyme-inhibitor complex. It provides information about the affinity of the inhibitor for the enzyme. The smaller the K_i value, the greater the affinity for the enzyme. The second parameter to study is the inactivation constant (k_{inact}).[55] This constant is a kinetic entity that provides the rate of inactivation that a molecule has for an enzyme. The inactivation process, (illustrated in **scheme 25**), suggests first of all an equilibrium towards the formation of a non-covalent and reversible enzyme-inhibitor complex. This complex (situation **B**) can then either dissociate and release the inhibitor (situation **A**) or react and irreversibly form a covalent enzyme-inhibitor complex (situation **C**).[56]

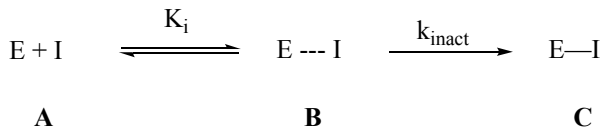

***Scheme 24**. Inactivation process of a glycosidase (**E**) in presence of an inhibitor (**I**)*

VI. EXPERIMENTAL PART

VI.1. Generalities

Molecular weights of different molecules have been determined with the software ChemDraw® 19.1 and 20.1

NMR spectra used for characterization of the synthesized molecules were recorded either on a JEOL JNM EX-400 (400 MHz for ^{1}H and 100 MHz for ^{13}C) or on a JEOL KNM EX-500 (500 MHz for ^{1}H and 126 MHz for ^{13}C) All spectra were realized in $CDCl_3$. The chemical shifts δ, are quoted in part per million (ppm) and calibrated with solvent residual peak ($CDCl_3$: ^{1}H 7.26 and ^{13}C 77.16 ppm). Each ^{1}H NMR spectrum is described as the following: chemical shift (ppm), multiplicity, coupling constant (Hz) and integration. Each ^{13}C NMR spectrum is described as the following: chemical shift (ppm) and multiplicity. The multiplicity is reported as following : s for singlet, d for doublet, t for triplet, q for quadruplet and m for multiplet. All spectra are analysed thanks to MestReNova® 14.2.1 and Delta® 6.0.0. Assignements were accomplished by COSY, HSQC and Noe experiments.

The carbons and corresponding hydrogens numbering follows the classical numbering of carbohydrate where the position 1 being the anomeric carbon. The numbering is described in **figure 17**.

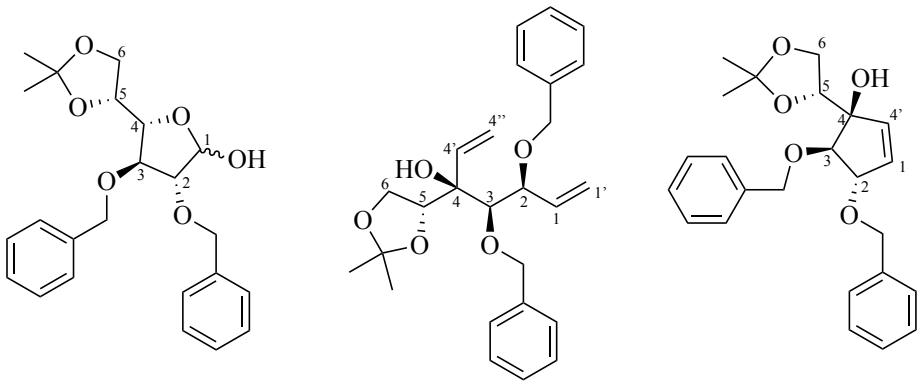

Figure 17. labelling of atoms used in NMR spectra

Reagents and chemicals were obtained from Merck, ABCR, Fischer, Acros at ACS grade and were used without any purification if not necessary. Toluene, dichloromethane, ethyl ether and tetrahydrofuran were taken from MB-SPS-800 taping machine brought from MBraun company. Distilled water was used for reactions work-up.

VI.2. Synthesis and protocols

VI.2.1. 5,6-*O*-isopropylidene-D-galactono-1,4-lactone

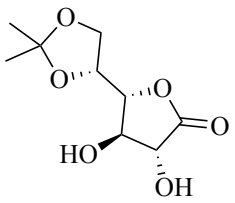

36

D-Galactose (10.00 g, 55.5 mmol, 1.0 equiv.) **35** and baryum carbonate (24.09 g, 122.1 mmol, 2.2 equiv.) were dissolved in water (50 mL) during 30 min. After, bromine (3.00 mL, 58.3 mmol, 1.05 equiv.) was added dropwise at 0 °C under argon atmosphere and stirred 6 h at room temperature. Sulfurous acid (0.44 mL, 5.55 mmol, 0.1 equiv.) was added to neutralize the remaining bromine. After 10 min, the solution was filtered through a plug of celite and washed with water to remove the salts. Then, filtrate was then concentrated under reduced pressure. The crude of D-galactono-1,4-lactone was dissolved in dry acetone under inert atmosphere of argon. p-toluene sulfonic acid (1.056 g, 5.55 mmol, 0.1 equiv.) and 2,2-dimethoxypropane (13.6 mL, 111.1 mmol, 2.0 equiv.) were added at 0 °C. The reaction was stirred overnight at room temperature. Then, the reaction was neutralized with sodium hydrogenocarbonate (0.468 g, 5.55 mmol, 0.1equiv.) and filtered through a plug of celite with acetone. A small amount of silica gel was added to the filtrate and the mixture was evaporated under reduced pressure. The purification by column chromatography (Cy/EtOAc 40:60) gave the expected product as a white solid **36** (5.6 g, 47 % over two steps). Known molecule. The analytical data corroborated with those published ones.[42]

- **Chemical formula:** $C_9H_{14}O_6$
- **Molecular weight:** 218.21 g/mol
- **R_f:** 0.17 (Cy/EtOAc 40:60)
- **Aspect:** White crystal
- **^{1}H NMR (500 MHz, Chloroform-*D*):** δ 4.44 (d, *J* = 7.4 Hz, 1H, H-2), 4.41 (dd, *J* = 7.5, *J* = 6.5 Hz, 1H, H-3), 4.39 (dd, *J* = 6.8, *J* = 3.2 Hz, 1H, H-5), 4.22 (dd, *J* = 6.3, *J* = 3.2 Hz, 1H, H-4), 4.15 (dd, *J* = 8.9, *J* = 6.9 Hz, 1H, H-6a), 4.02 (dd, *J* = 8.7, *J* = 6.7 Hz, 1H, H-6b), 1.43 (s, 3H, C*H*$_3$), 1.39 (s, 3H, C*H*$_3$) ppm.
- **^{13}C NMR (126 MHz, Chloroform-*D*):** δ 173.4 (C-1), 110.9 (*C*(CH$_3$)$_2$), 76.7 (C-3), 75.1 (C-2), 75.0 (C-4), 74.1 (C-5), 65.4 (C-6), 26.3 (*C*H$_3$), 25.8 (*C*H$_3$) ppm.

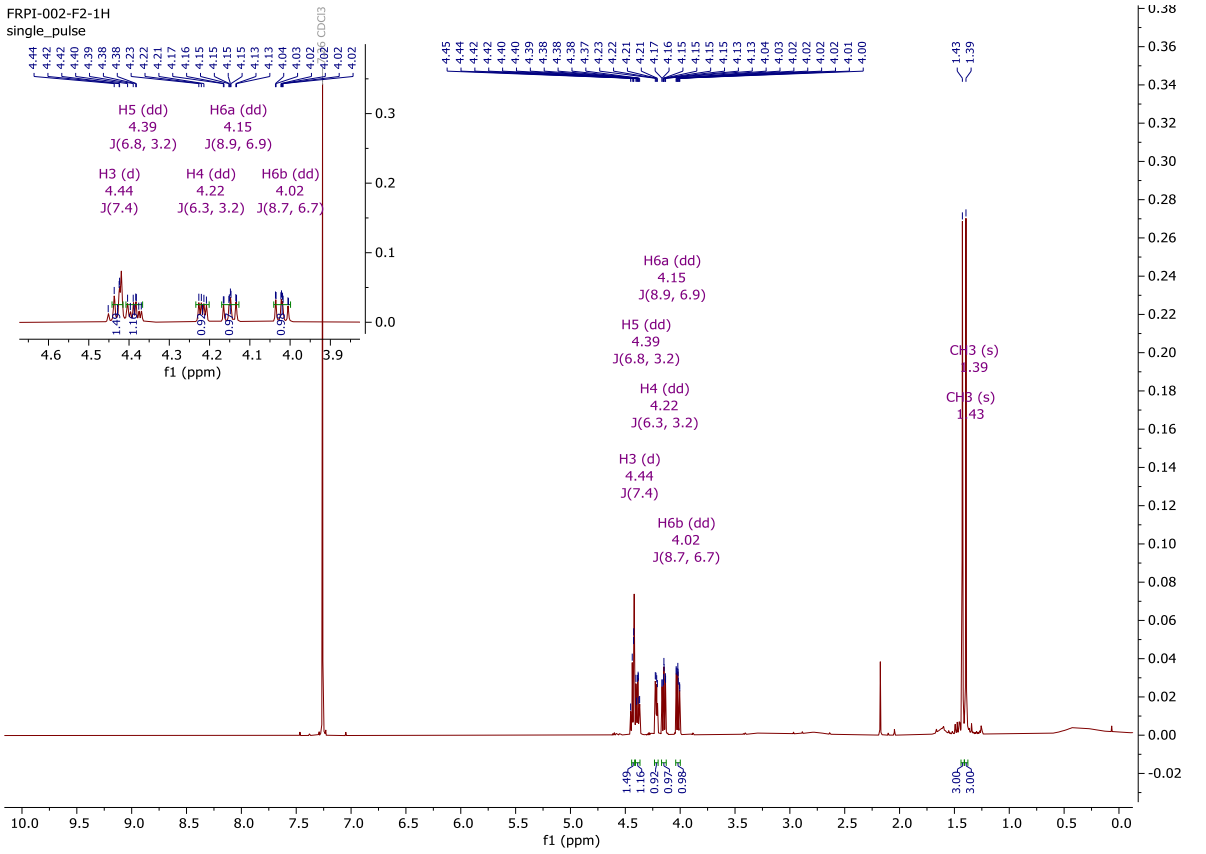
FRPI-002-F2-1H
single_pulse
H5 (dd)
4.39
J(6.8, 3.2)
H6a (dd)
4.15
J(8.9, 6.9)
H3 (d)
4.44
J(7.4)
H4 (dd)
4.22
J(6.3, 3.2)
H6b (dd)
4.02
J(8.7, 6.7)
CH3 (s)
1.39
CH3 (s)
1.43
f1 (ppm)

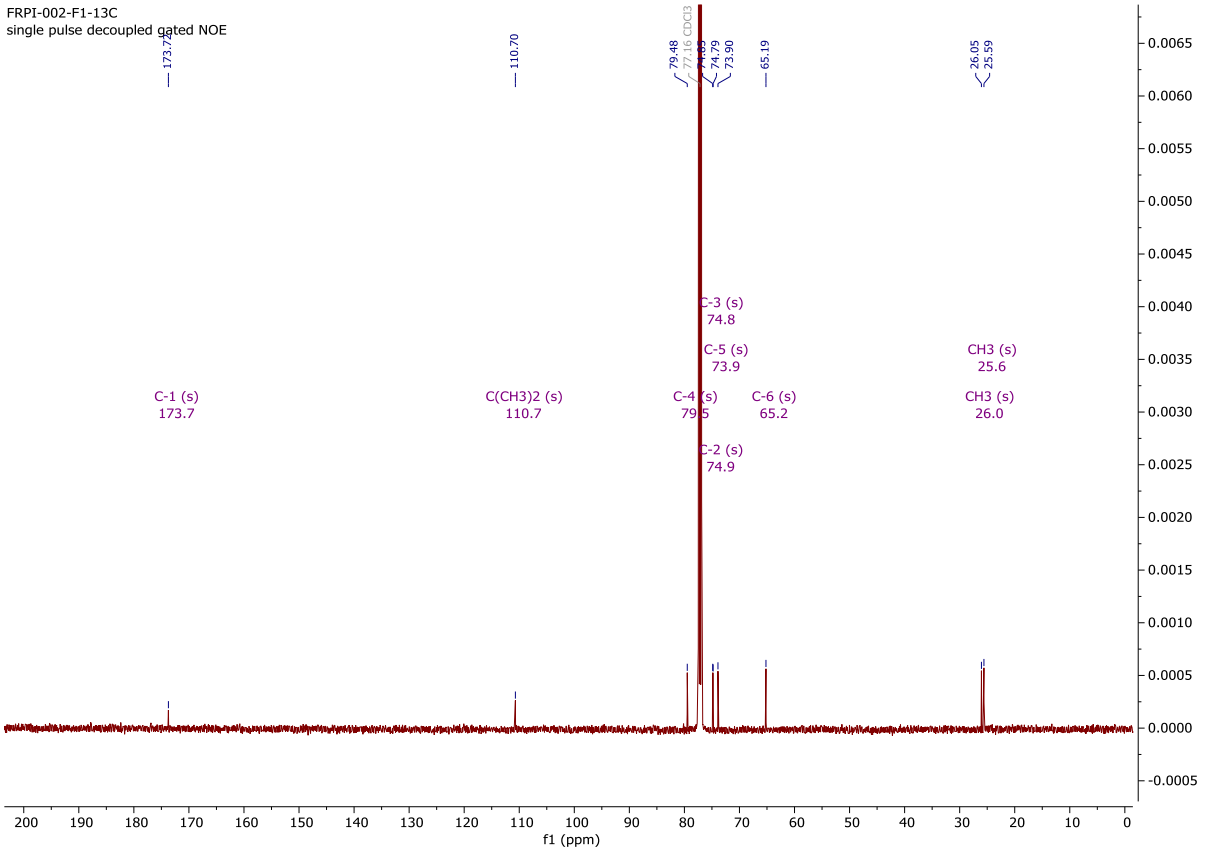
FRPI-002-F1-13C
single pulse decoupled gated NOE
C-1 (s)
173.7
C(CH3)2 (s)
110.7
C-3 (s)
74.8
C-5 (s)
73.9
C-4 (s)
79.5
C-6 (s)
65.2
C-2 (s)
74.9
CH3 (s)
25.6
CH3 (s)
26.0
f1 (ppm)

VI.2.2. 2,3-Di-*O*-benzyl-5,6-*O*-isopropylidene-D-galactono-1,4-lactone

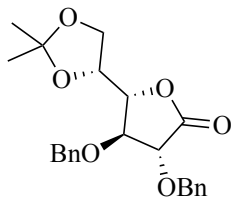

37

To a solution of 5,6-*O*-isopropylidene-D-galactono-1,4-lactone **36** (8.00 g, 36.6 mmol) in dry acetonitrile (160 mL) was added benzyl bromide (47.1 mL, 397 mmol, 11 equiv.) at room temperature under inert atmosphere of argon. Silver (I) oxyde (33.92 g, 146 mmol, 4 equiv.) was added in two parts over 12 h. The flask was covered by aluminium foil and the reaction was stirred at room temperature for 24 h. The reaction mixture was then filtered through a celite pad and the resulting cake was washed with acetonitrile. The filrate was concentred under vacuum and purified by column chromatography (Cy/EtOAc 99:1 until Cy/EtOAc 80:20) to give product **37** (8.43 g, 58 %). Known molecule. The analytical data corroborated with those published ones.[42]

- **Chemical formula:** $C_{23}H_{26}O_6$
- **Molecular weight:** 398.46 g/mol
- **Rf:** 0.25 (Cy/EtOAc 8:2)
- **Aspect:** White powder
- **^{1}H NMR (500 MHz, Chloroform-*D*) :** δ 7.46 – 7.26 (m, 10H, H arom.), 5.11 (d, *J* = 11.5 Hz, 1H, C*H*$_2$Ph), 4.79 (d, *J* = 11.4 Hz, 1H, C*H*$_2$Ph), 4.66 (d, *J* = 11.5 Hz, 1H, C*H*$_2$Ph), 4.56 (d, *J* = 11.5 Hz, 1H, C*H*$_2$Ph), 4.36 (d, *J* = 7.4 Hz, 1H, H-2), 4.32 (t, *J* = 7.2 Hz, 1H, H-3), 4.21 (td, *J* = 6.7, *J* = 3.4 Hz, 1H, H-5), 4.15 (dd, *J* = 7.1, *J* = 3.7 Hz, 1H, H-4), 4.01 (dd, *J* = 8.6, *J* = 6.7 Hz, 1H, H-6b), 3.93 (dd, *J* = 8.5, *J* = 6.8 Hz, 1H, H-6a), 1.40 (s, 3H, C*H*$_3$), 1.35 (s, 3H, C*H*$_3$) ppm.
- **^{13}C NMR (126 MHz, Chloroform-*D*) :** δ 172.4 (C-1), 137.0 (Cq arom.), 136.8 (Cq arom.), 128.9 – 128.1 (C-H arom.), 110.4 (*C*(CH$_3$)$_2$), 79.6 (C-3), 79.2 (C-2), 78.7 (C-4), 74.5 (C-5), 72.9 (CH$_2$Ph), 72.6 (CH$_2$Ph), 65.2 (C-6), 26.2 (*C*H$_3$), 25.7 (*C*H$_3$) ppm.

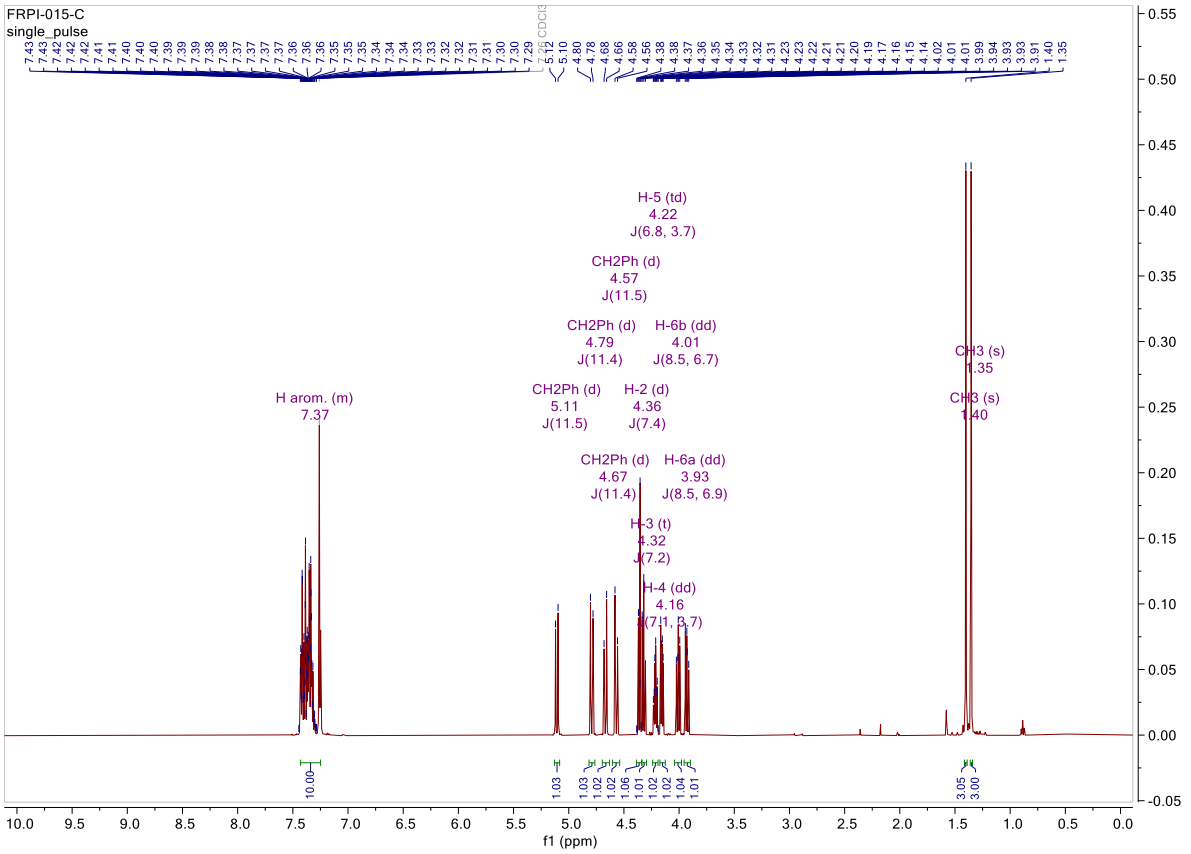
FRPI-015-C
single_pulse
H-5 (td)
4.22
J(6.8, 3.7)
CH2Ph (d)
4.57
J(11.5)
CH2Ph (d)
4.79
J(11.4)
H-6b (dd)
4.01
J(8.5, 6.7)
CH3 (s)
1.35
CH2Ph (d)
5.11
J(11.5)
H-2 (d)
4.36
J(7.4)
H arom. (m)
7.37
CH3 (s)
1.40
CH2Ph (d)
4.67
J(11.4)
H-6a (dd)
3.93
J(8.5, 6.9)
H-3 (t)
4.32
J(7.2)
H-4 (dd)
4.16
J(7.1, 3.7)
f1 (ppm)

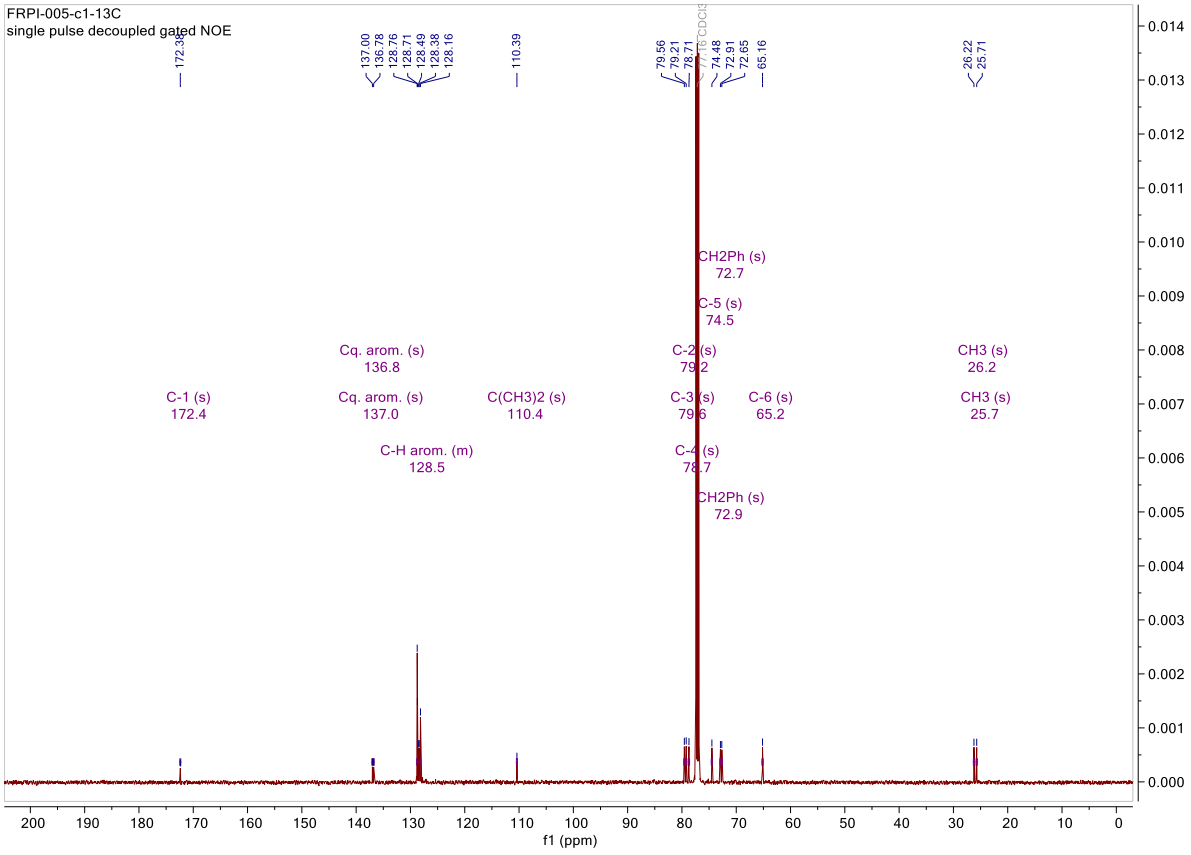
FRPI-005-c1-13C
single pulse decoupled gated NOE
CH2Ph (s)
72.7
C-5 (s)
74.5
Cq. arom. (s)
136.8
C-2 (s)
79.2
CH3 (s)
26.2
C-1 (s)
172.4
Cq. arom. (s)
137.0
C(CH3)2 (s)
110.4
C-3 (s)
79.6
C-6 (s)
65.2
CH3 (s)
25.7
C-H arom. (m)
128.5
C-4 (s)
78.7
CH2Ph (s)
72.9
f1 (ppm)

VI.2.3. 2,3-Di-*O*-benzyl-5,6-*O*-isopropylidene-D-galactofuranose

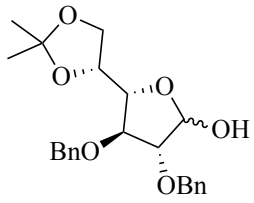

38

2,3-Di-*O*-benzyl-5,6-*O*-isopropylidene-D-galactono-1,4-lactone **37** (0.240 g, 0.6 mmol) is dissolved in dry dichloromethane (4.00 mL) under inert atmosphere of argon. Then, at -78 °C, diisobutylaluminium hydride (0.76 mL, 0.76 mmol, 1.25 equiv.) was added dropwise and the reaction mixture was stirred at room temperature during 4 h. After a second addition of diisobutylaluminium hydride (0.15 mL, 0.15 mmol, 0.25 equiv.), the mixture was stirred at room temperature during 1 h. Methanol (0.9 mL) and a saturated solution of sodium potassium tartrate (2.27 mL) were added and the mixture was stirred during 1 h. Water (2 mL) and ethyl acetate (1.81 mL) were added. The organic phase was separated and the aqueous phase was extracted three times with ethyl acetate. The organic extracts were gathered, dried with magnesium sulfate, filtered and concentrated under reduced pressure. The crude obtained was purified by column chromatography (Cy/EtOAc 70:30) to give product **38** (0.185 g, 77 %). Known molecule. The analytical data corroborated with those published ones.[42]

- **Chemical formula:** $C_{23}H_{28}O_6$
- **Molecular weight:** 400.47 g/mol
- **R_f:** 0.30 (Cy/EtOAc 70:30)
- **Aspect:** White solid / colorless oil
- **^{1}H NMR (500 MHz, Chloroform-*D*):** δ 7.38 – 7.28 (m, 10H, H arom), 5.45 (d, *J* = 5.9 Hz, 1H, H-1β), 5.33 (dd, *J* = 9.7, *J* = 4.2 Hz, 1H, H-1α), 4.70 (d, *J* = 11.5 Hz, 2H, C*H*$_2$Ph), 4.67 (d, *J* = 11.7 Hz, 1H, C*H*$_2$Ph), 4.63 (d, *J* = 11.8 Hz, 1H, CH$_2$Ph), 4.57 (d, *J* = 11.9 Hz, 1H, C*H*$_2$Ph), 4.54 (d, *J* = 12.0 Hz, 1H, C*H*$_2$Ph), 4.52 (d, *J* = 11.9 Hz, 1H, C*H*$_2$Ph), 4.47 (d, *J* = 11.9 Hz, 1H, C*H*$_2$Ph), 4.23 (dd, *J* = 7.2, *J* = 4.7 Hz, H-5α), 4.20 (d, *J* = 6.5 Hz, 1H, H-5β), 4.02 (m, H-2 α/β), 3.85 (dd, *J* = 8.5, *J* = 6.5 Hz, 1H, H-6b α/β), 3.67 (dd, *J* = 9.7, *J* = 3.6 Hz, 1H, OHα), 2.98 (s, 1H, OHβ), 1.43 (s, 3H, C*H*$_3$), 1.42 (s, 3H, C*H*$_3$)., 1.35 (s, 3H, C*H*$_3$), 1.35 (s, 3H, C*H*$_3$) ppm.
- **^{13}C NMR (126 MHz, Chloroform-*D*):** δ 137.7 (Cq arom. β), 137.3 (Cq arom. α), 137.3 (Cq arom. β), 137.1 (Cq arom. α), 128.8 – 128.0 (C-H arom.), 109.9 (*C*(CH$_3$)$_2$), 101.1

(C-1β), 96.1 (C-1α), 86.9 (C-2β), 84.0 (C-2α), 83.8 (C-3β), 83.2 (C-4β), 81.9 (C-3α), 80.3 (C-4α), 76.3 (C-5), 72.5 (*C*H_2Ph β), 72.4 (*C*H_2Ph β), 72.3 (*C*H_2Ph α), 72.1 (*C*H_2Ph α), 65.6 (C-6), 26.7 (*C*H_3 β), 26.4 (*C*H_3 α), 25.§ (*C*H_3 β), 25.4 (*C*H_3 α) ppm.

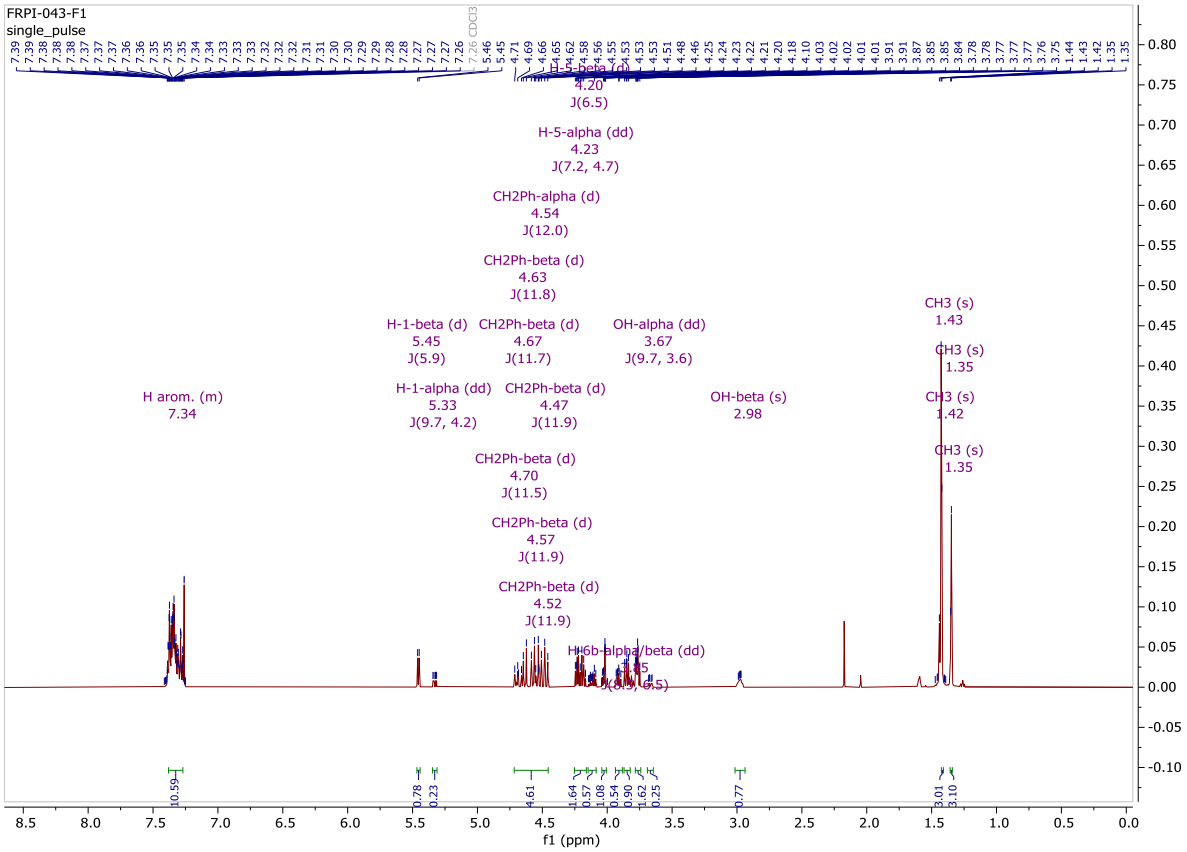

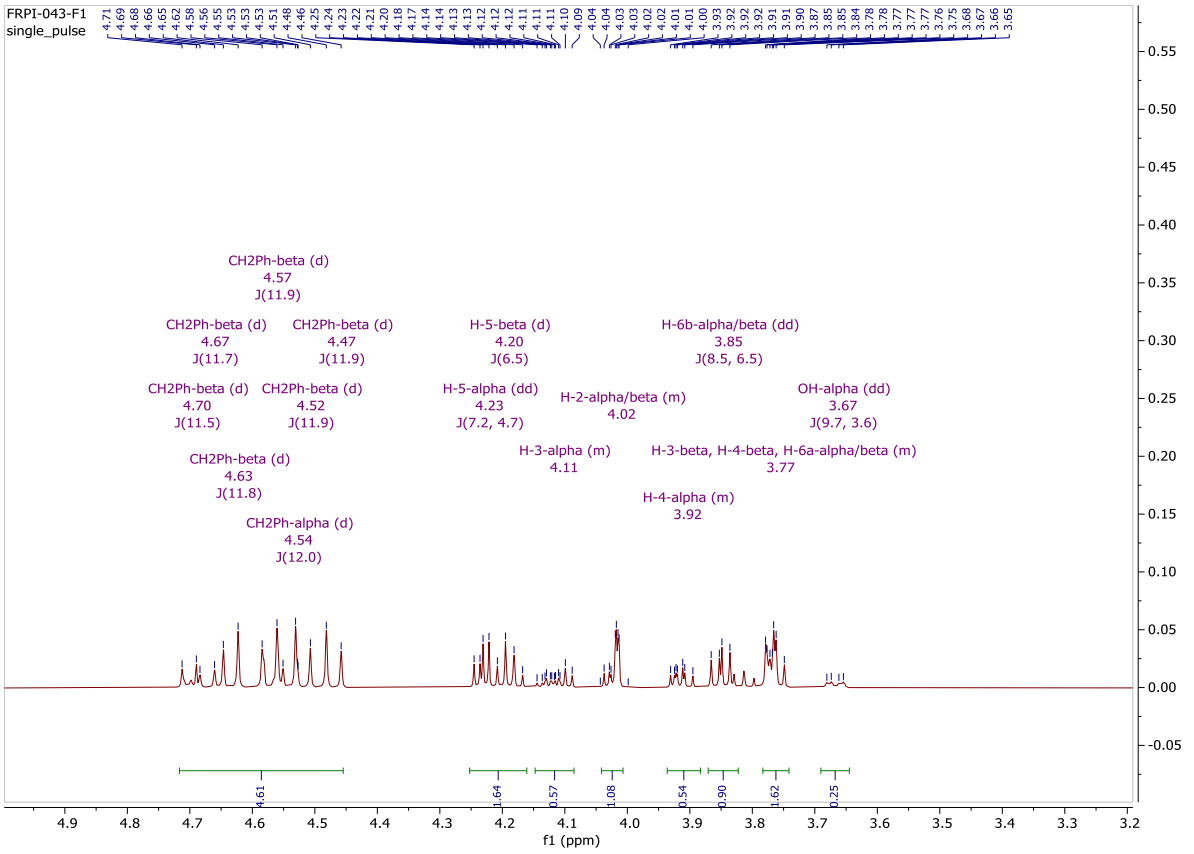
FRPI-043-F1
single_pulse
CH2Ph-beta (d)
4.57
J(11.9)
CH2Ph-beta (d)
4.67
J(11.7)
CH2Ph-beta (d)
4.47
J(11.9)
H-5-beta (d)
4.20
J(6.5)
H-6b-alpha/beta (dd)
3.85
J(8.5, 6.5)
CH2Ph-beta (d)
4.70
J(11.5)
CH2Ph-beta (d)
4.52
J(11.9)
H-5-alpha (dd)
4.23
J(7.2, 4.7)
H-2-alpha/beta (m)
4.02
OH-alpha (dd)
3.67
J(9.7, 3.6)
H-3-alpha (m)
4.11
H-3-beta, H-4-beta, H-6a-alpha/beta (m)
3.77
CH2Ph-beta (d)
4.63
J(11.8)
H-4-alpha (m)
3.92
CH2Ph-alpha (d)
4.54
J(12.0)
f1 (ppm)

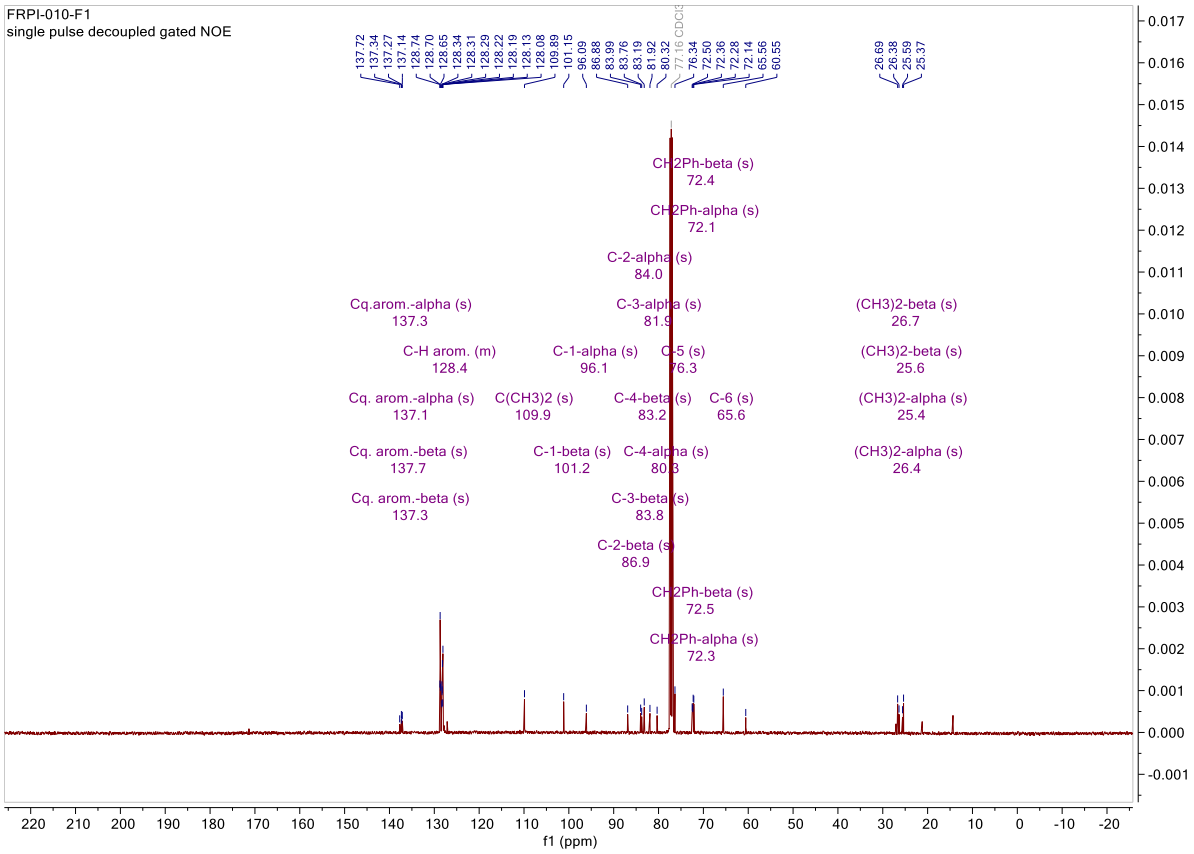
FRPI-010-F1
single pulse decoupled gated NOE
CH2Ph-beta (s)
72.4
CH2Ph-alpha (s)
72.1
C-2-alpha (s)
84.0
Cq.arom.-alpha (s)
137.3
C-3-alpha (s)
81.9
(CH3)2-beta (s)
26.7
C-H arom. (m)
128.4
C-1-alpha (s)
96.1
C-5 (s)
76.3
(CH3)2-beta (s)
25.6
Cq. arom.-alpha (s)
137.1
C(CH3)2 (s)
109.9
C-4-beta (s)
83.2
C-6 (s)
65.6
(CH3)2-alpha (s)
25.4
Cq. arom.-beta (s)
137.7
C-1-beta (s)
101.2
C-4-alpha (s)
80.3
(CH3)2-alpha (s)
26.4
Cq. arom.-beta (s)
137.3
C-3-beta (s)
83.8
C-2-beta (s)
86.9
CH2Ph-beta (s)
72.5
CH2Ph-alpha (s)
72.3
f1 (ppm)

VI.2.4. 2,3-Di-*O*-benzyl-1,1'-dideoxy-5,6-*O*-isopropylidene-D-galacto-hept-1'-enitol

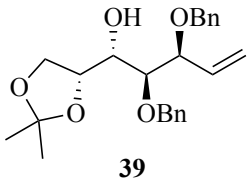

39

To a suspension of the 2,3-Di-*O*-benzyl-5,6-*O*-isopropylidene-D-galactofuranose **38** (5.41 g, 13.6 mmol) in dry tetrahydrofuran (70 mL) was added dropwise a 2.5 M solution of n-butyllithium in hexane (5.43 mL, 13.6 mmol, 1 equiv.) at -78 °C under inert atmosphere of argon and the reaction was stirred 30 min at 0 °C. In another flask, phoshonium ylide was prepared with methyltriphenylphosphonium bromide (14.55 g, 40.7 mmol, 3 equiv.) in dry tetrahydrofuran (140 mL) and the addition of a 2.5 M solution of n-butyllithium in hexane (15.2 mL, 38 mmol, 2.8 equiv.) at -78 °C under inert atmosphere of argon. The reaction was stirred 30 min at 0 °C. Then, the flask containig the suspension of 2,3-Di-*O*-benzyl-5,6-*O*-isopropylidene-D-galactofuranose **38** was transferred by cannula into the flask containing the ylide and the reaction was stirred for 3 h at room temperature. The reaction was quenched with a saturated solution of ammonium chloride (36 mL). The mixture was diluted with ethyl acetate (18 mL) and water (18 mL). The organic phase was separated and aqueous phase was extracted with ethyl acetate (80 mL). The organic phases were gathered, dried with magnesium sulfate, filtered and concentrated under reduced pressure. The crude was purified by column chromatography (Cy/EtOAc 80:20) to give the expected product (**39**) (3.67 g, 68 %). Known molecule. The analytical data corroborated with those published ones.[42]

- **Chemical formula:** $C_{24}H_{30}O_5$
- **Molecular weight:** 398.50 g/mol
- **Rf:** 0.49 (Cy/EtOAc 80:20)
- **Aspect:** Orange oil
- **^{1}H NMR (500 MHz, Chloroform-*D*):** δ 7.38 – 7.28 (m, 10H, H arom.), 6.00 (ddd, *J* = 17.6, *J* = 10.4, *J* = 7.5 Hz, 1H, H-1), 5.37 (dd, *J* = 14.6, *J* = 1.4 Hz, 1H, H-1'a), 5.34 (dd, *J* = 7.6 , *J* = 1.3 Hz, 1H, H-1'b), 4.67 (d, *J* = 11.2 Hz, 1H, C*H*$_2$Ph), 4.65 (d, *J* = 11.8 Hz, 1H, C*H*$_2$Ph), 4.58 (d, *J* = 11.3 Hz, 1H, C*H*$_2$Ph), 4.40 (d, *J* = 11.9 Hz, 1H, C*H*$_2$Ph), 4.30 (ddd, *J* = 7.1 *J* = 6.6 , *J* = 3.0 Hz, 1H, H-5), 4.18 (dd, *J* = 7.5 , *J* = 3.1 Hz, 1H, H-2), 3.97 (dd, *J* = 7.8, *J* = 6.6 Hz, 1H, H-6b), 3.88 (dd, *J* = 8.4, *J* = 6.8 Hz, 1H, H-6a),

3.77 (ddd, *J* = 3.0, *J* = 6.7, *J* = 3.1 Hz, 1H, H-4), 3.52 (dd, *J* = 8.4, *J* = 3.1 Hz, 1H, H-3), 2.61 (d, *J* = 6.6 Hz, 1H, OH), 1.43 (s, 3H, CH_3), 1.35 (s, 3H, CH_3) ppm.

- **^{13}C NMR (126 MHz, Chloroform-*D*) :** δ 207.6 (C-4), 137.7 (Cq arom.), 137.1 (Cq arom.), 134.5 (C-1), 128.8 – 128.0 (C-H arom.), 120.0 (C-1'), 110.8 (*C*$(CH_3)_2$), 86.0 (C-3), 81.0 (C-2), 79.2 (C-5), 75.1 (*C*H_2Ph), 71.2 (*C*H_2Ph), 65.6 (C-6), 26.1 (*C*H_3), 25.6 (*C*H_3) ppm.

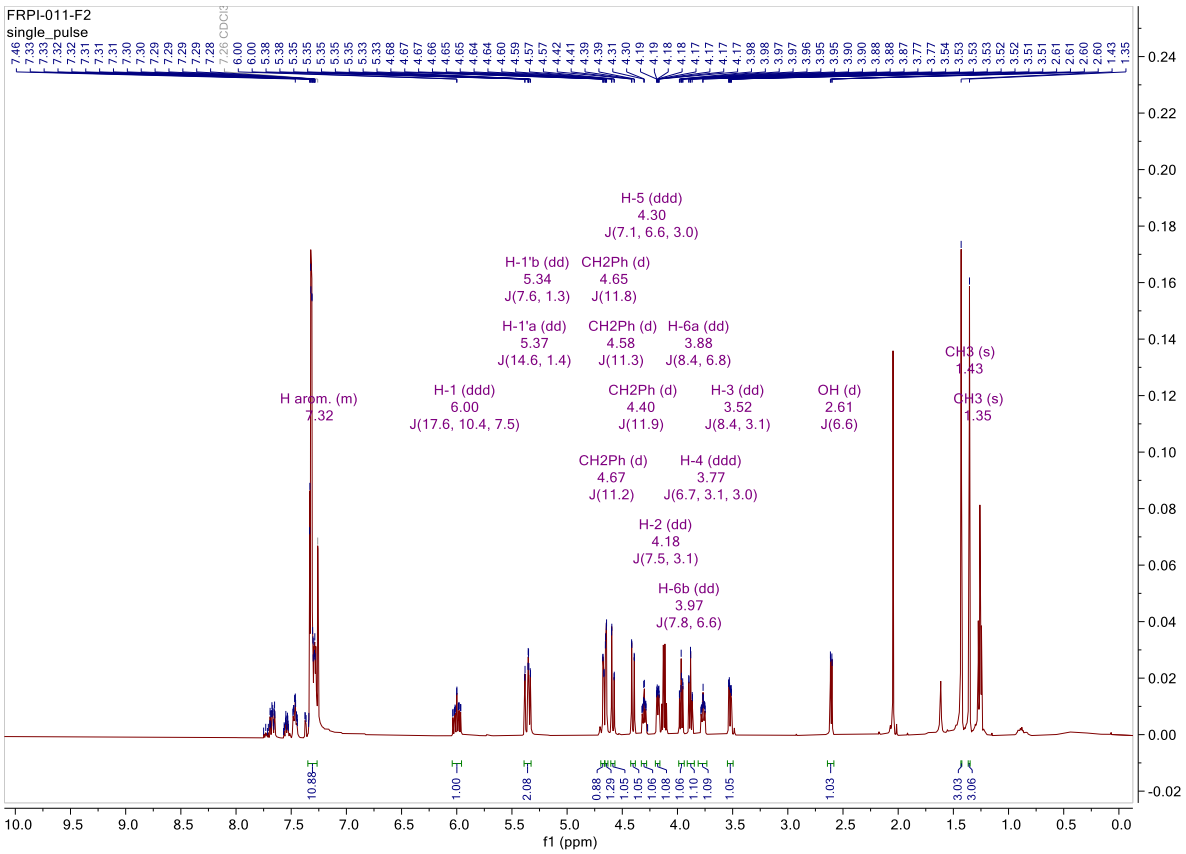

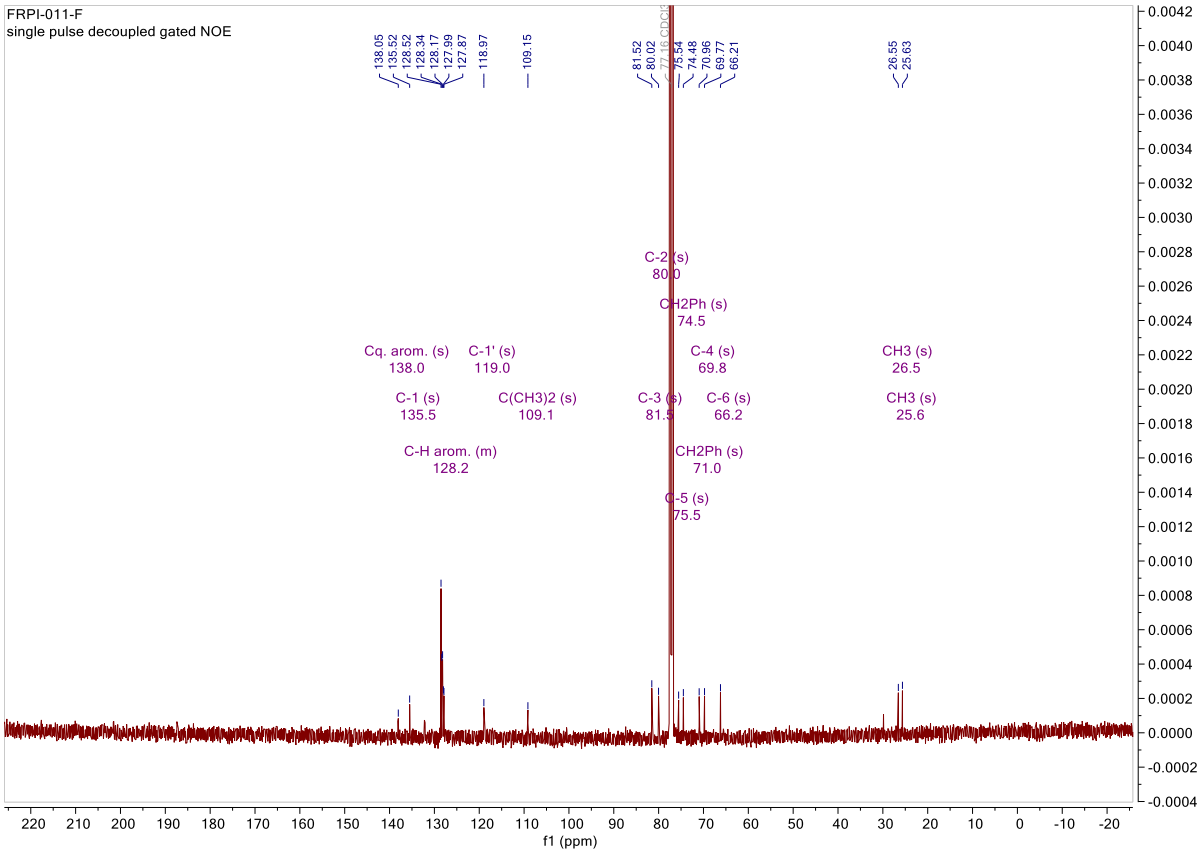
FRPI-011-F
single pulse decoupled gated NOE
138.05
135.52
128.52
128.34
128.17
127.99
127.87
118.97
109.15
81.52
80.02
77.16 CDCl3
75.54
74.48
70.96
69.77
66.21
26.55
25.63
C-2 (s)
80.0
CH2Ph (s)
74.5
Cq. arom. (s)
138.0
C-1' (s)
119.0
C-4 (s)
69.8
CH3 (s)
26.5
C-1 (s)
135.5
C(CH3)2 (s)
109.1
C-3 (s)
81.5
C-6 (s)
66.2
CH3 (s)
25.6
C-H arom. (m)
128.2
CH2Ph (s)
71.0
C-5 (s)
75.5
f1 (ppm)

VI.2.5. 2,3-Di-*O*-benzyl-1,1'-dideoxy-5,6-*O*-isopropylidene-D-galacto-hept-1'-en-4-one

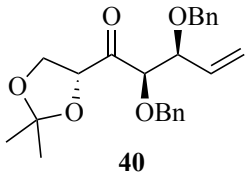

40

To a solution of 2,3-Di-*O*-benzyl-1,1'-dideoxy-5,6-*O*-isopropylidene-D-galacto-hept-1'-enitol **39** (0.41 g, 1.0 mmol) in dry dichloromethane (6.1 mL) at 0 °C was added Dess-Martin periodinane (0.49 g, 1.16 mmol, 1.5 equiv.). After addition, the reaction was allowed to reach room temperature and stirred for 2 h. Saturated sodium hydrogenocarbonate solution (5.3 mL) and saturated sodium thiosulfate solution (2.6 mL) were added. The organic layer was separated and the aqueous layer was extracted three times with dichloromethane (5 mL). The organic layers were gathered, dried with magnesium sulfate, filtered and concentrated under reduced pressure. The resulting oil obtained was purified by column chromatography (Cy/EtOAc 90:10) to afford product **40** (144 mg, 35 %).

- **Chemical formula:** $C_{24}H_{28}O_5$
- **Molecular weight:** 396.48 g/mol
- **Rf:** 0.27 (Cy/EtOAc 90:10)
- **Aspect:** Yellow oil
- **^{1}H NMR (500 MHz, Chloroform-*D*):** δ 7.35 – 7.27 (m, 10H, H arom), 5.93 (ddd, *J* = 17.5, *J* = 10.3, *J* = 7.8 Hz, 1H, H-1), 5.38 (dt, *J* = 17.4, *J* = 1.1 Hz, 1H, H-1'a), 5.34 (dd, *J* = 10.9 , *J* = 1.6 Hz, 1H, H-1'b), 4.79 (dd, *J* = 7.6 *J* = 6.5 Hz, 1H, H-5), 4.66 (d, *J* = 11.6 Hz, 1H, C*H*$_2$Ph), 4.62 (d, *J* = 11.6 Hz, 1H, C*H*$_2$Ph), 4.57 (d, *J* = 11.6 Hz, 1H, C*H*$_2$Ph), 4.29 (d, *J* = 11.7 Hz, 1H, C*H*$_2$Ph), 4.14 (m, 2H, H-6), 4.07 (d, *J* = 3.4 Hz, 1H, H-3), 1.44 (s, 3H, C*H*$_3$), 1.38 (s, 3H, C*H*$_3$) ppm.
- **^{13}C NMR (126 MHz, Chloroform-*D*):** δ 207.4 (C-4), 137.5 (Cq arom.), 136.9 (Cq arom.), 134.3 (C-1), 128.8 – 128.0 (C-H arom.), 119.8 (C-1'), 110.6 (*C*(CH$_3$)$_2$), 85.8 (C-3), 80.8 (C-2), 79.0 (C-5), 74.9 (*C*H$_2$Ph), 71.0 (*C*H$_2$Ph), 65.4 (C-6), 25.9 (*C*H$_3$), 25.4 (*C*H$_3$) ppm.
- **HRMS (ESI):** m/z calculated for $C_{24}H_{28}O_5$ $[M+Na]^+$: 419.1829; found: 419.1827; δ = 0.2 ppm

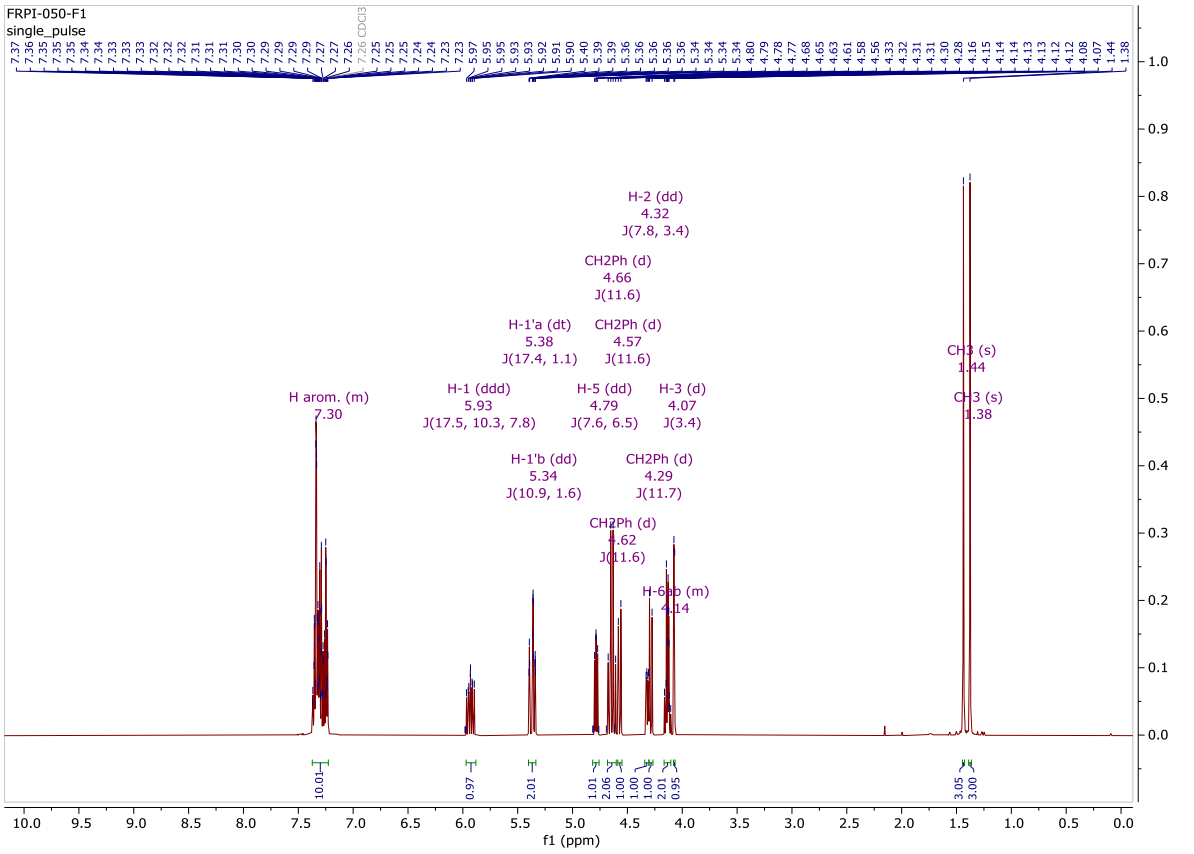
FRPI-050-F1
single_pulse
H-2 (dd)
4.32
J(7.8, 3.4)
CH2Ph (d)
4.66
J(11.6)
H-1'a (dt)
5.38
J(17.4, 1.1)
CH2Ph (d)
4.57
J(11.6)
CH3 (s)
1.44
H arom. (m)
7.30
H-1 (ddd)
5.93
J(17.5, 10.3, 7.8)
H-5 (dd)
4.79
J(7.6, 6.5)
H-3 (d)
4.07
J(3.4)
CH3 (s)
1.38
H-1'b (dd)
5.34
J(10.9, 1.6)
CH2Ph (d)
4.29
J(11.7)
CH2Ph (d)
4.62
J(11.6)
H-6ab (m)
4.14
f1 (ppm)

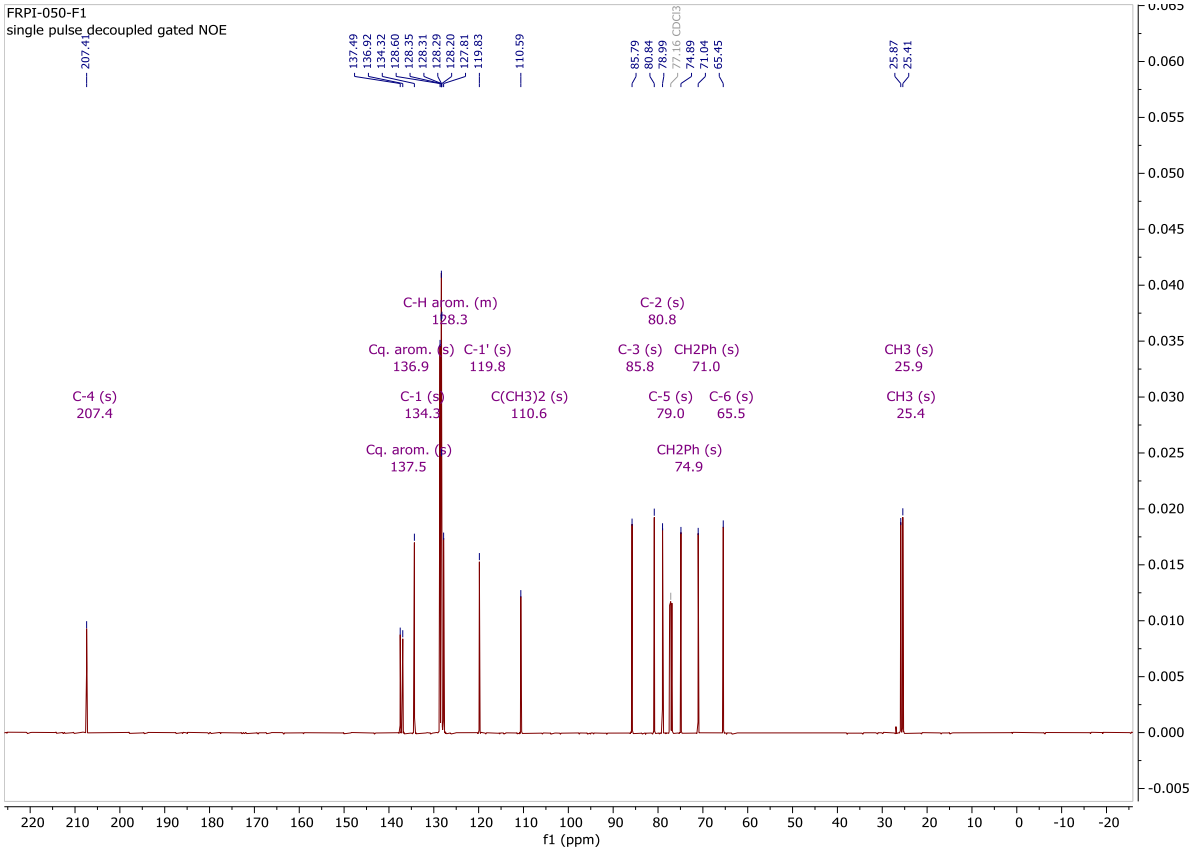
FRPI-050-F1
single pulse decoupled gated NOE
C-H arom. (m)
128.3
C-2 (s)
80.8
Cq. arom. (s)
136.9
C-1' (s)
119.8
C-3 (s)
85.8
CH2Ph (s)
71.0
CH3 (s)
25.9
C-4 (s)
207.4
C-1 (s)
134.3
C(CH3)2 (s)
110.6
C-5 (s)
79.0
C-6 (s)
65.5
CH3 (s)
25.4
Cq. arom. (s)
137.5
CH2Ph (s)
74.9
f1 (ppm)

VI.2.6. 2,3-Di-*O*-benzyl-4,4'-didehydro-1,1',4,4'-tetradeoxy-5,6-*O*-isopropylidene-D-galacto-hept-1'-en-4-ol

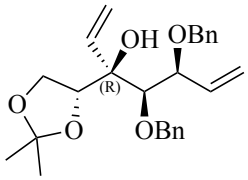

R-41

To a solution 2,3-Di-*O*-benzyl-1,1'-dideoxy-5,6-*O*-isopropylidene-D-galacto-hept-1'-en-4-one **40** (0.135 g, 0.34 mmol) in dry THF (1.05 mL) was added dropwise vinylmagnesium bromide, (0.345 mL, 1.0 M solution in THF, 0.345 mmol, 1.5 equiv.) at -78°C. After addition, the reaction was stirred for 15 min at the same temperature then at -20°C for 1 h. After, saturated solution of ammonium chloride and brine were added. The aqueous layer was separated and extracted with EtOAc. The organic layers were gathered, dried with magnesium sulfate and concentrated under reduced pressure. The resulting residue was purified by column chromatography (Cy/EtOAc 80:20) to afford product **R-41** (61 mg, 42 %).

- **Chemical formula:** $C_{26}H_{32}O_5$
- **Molecular weight:** 425.54 g/mol
- **Rf:** 0.18 (Cy/EtOAc 80:20)
- **Aspect:** Yellow oil
- **^{1}H NMR (500 MHz, Chloroform-*D*):** δ 7.46 – 7.27 (m, 10H, H arom), 6.01 (ddd, *J* = 17.5, *J* = 10.3, *J* = 7.8 Hz, 1H, H-1), 5.94 (dd, *J* = 17.5, *J* = 11.1 Hz, 1H, H-4'), 5.42 (dd, *J* = 17.2, *J* = 2.1 Hz, 1H, H-4"a), 5.34 (dd, *J* = 12.8 , *J* = 1.2 Hz, 1H, H-1'a), 5.31 (dd, *J* = 9.1 , *J* = 2.1 Hz, 1H, H-1'b), 5.29 (dd, *J* = 9.1 , *J* = 1.7 Hz, 1H, H-4"b), 4.81 (d, *J* = 10.9 Hz, 1H, C*H*$_2$Ph), 4.73 (d, *J* = 11.0 Hz, 1H, C*H*$_2$Ph), 4.58 (m, 1H, H-3), 4.55 (d, *J* = 10.1 Hz, 1H, C*H*$_2$Ph), 4.48 (t, *J* = 6.5 Hz, 1H, H-5), 4.20 (dd, *J* = 8.0, *J* = 2.0 Hz, 1H, H-2), 4.19 (d, *J* = 11.1 Hz, 1H, C*H*$_2$Ph), 3.98 (dd, *J* = 8.5, *J* = 6.9 Hz, 1H, H-6a), 3.78 (dd, *J* = 8.4, *J* = 6.0 Hz, 1H, H-6b), 3.68 (d, *J* = 2.1 Hz, 1H, OH), 1.41 (s, 3H, C*H*$_3$), 1.33 (s, 3H, C*H*$_3$) ppm.
- **^{13}C NMR (126 MHz, Chloroform-*D*):** δ), 138.2 (Cq arom.), 137.1 (Cq arom.), 136.8 (C-4'), 135.9 (C-1), 128.8 (C-H arom.), 128.6 (C-H arom.), 128.5 (C-H arom.), 128.5 (C-H arom.), 128.2 (C-H arom.), 127.9 (C-H arom.), 119.1 (C-1'), 117.1 (C-4"), 109.2 (*C*(CH$_3$)$_2$), 82.4 (C-2), 81.5 (C-3), 80.0 (C-4), 76.3 (C-5), 75.9 (*C*H$_2$Ph), 70.7 (*C*H$_2$Ph), 65.4 (C-6), 26.3 (*C*H$_3$), 24.8 (*C*H$_3$) ppm.

- **HRMS (ESI):** m/z calculated for $C_{26}H_{32}O_5$ $[M+Na]^+$: 447.21420; found: 447.21393; δ = 0.6 ppm

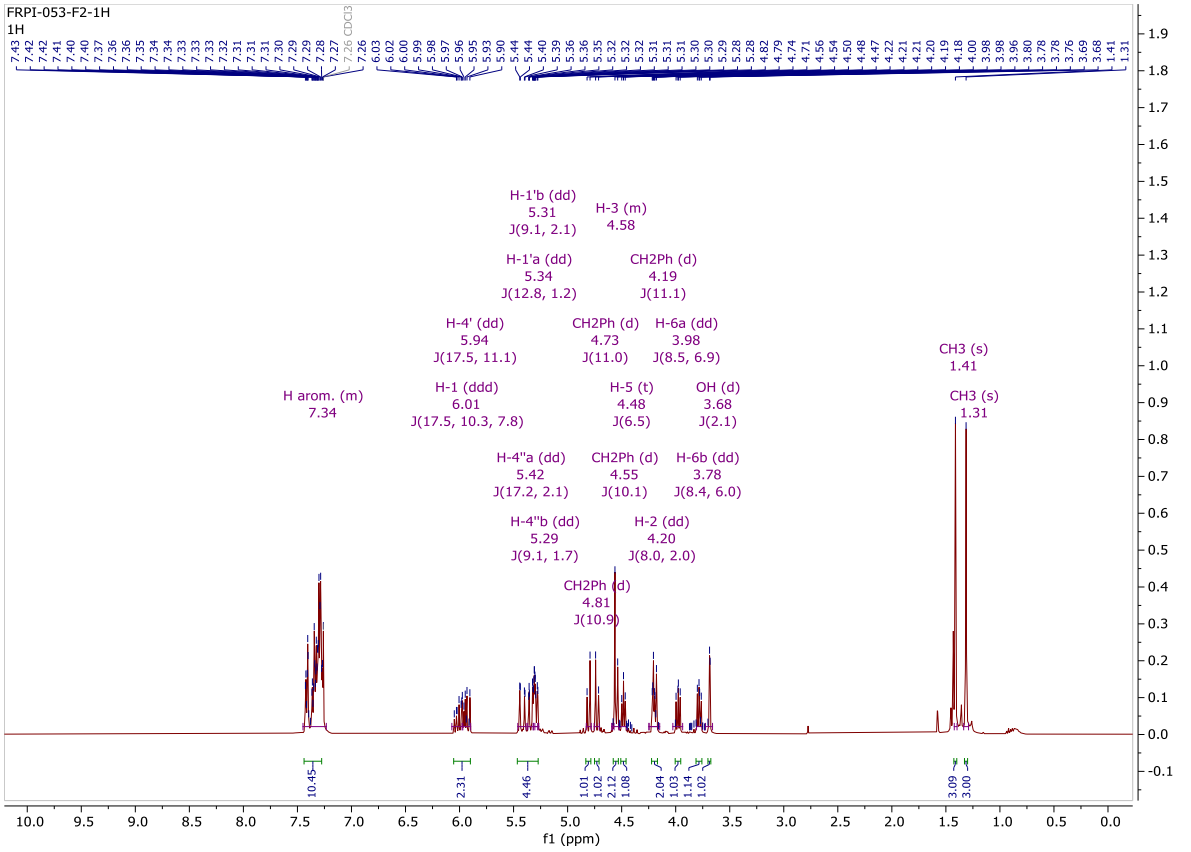

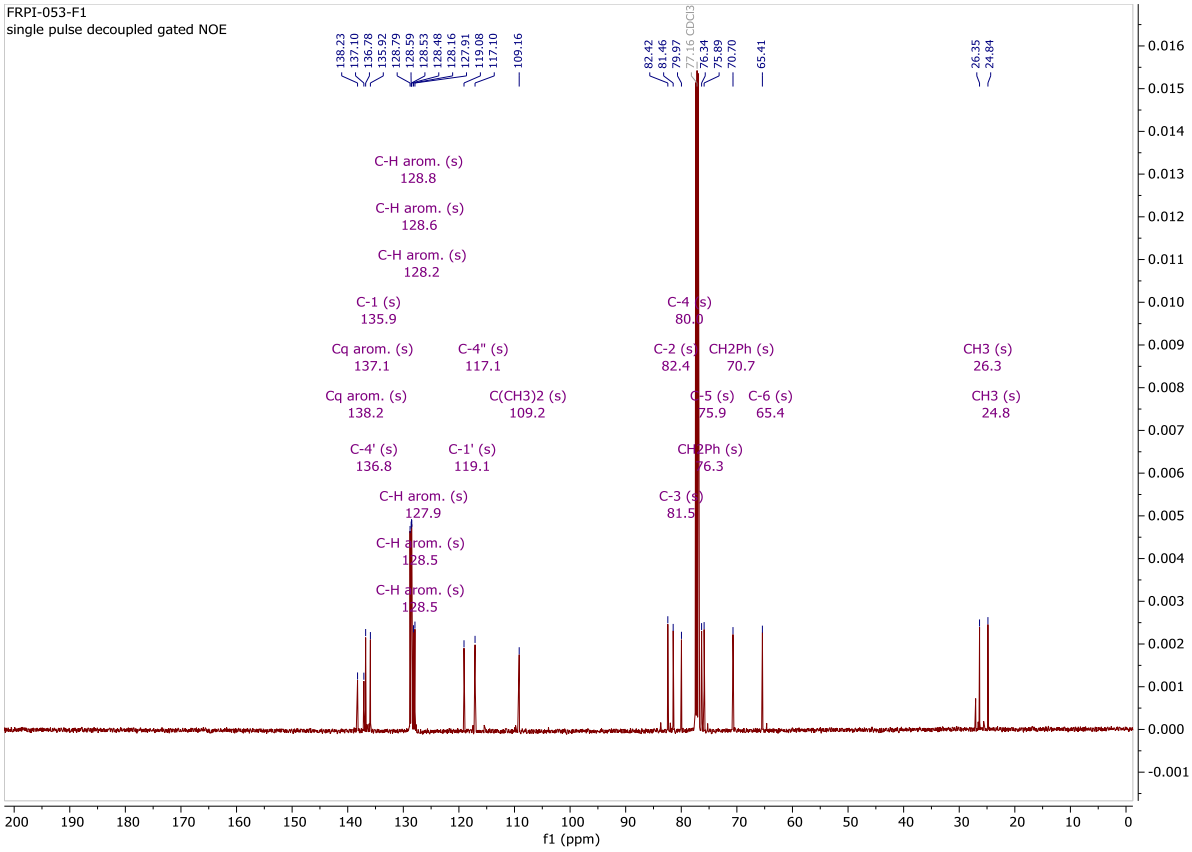

VI.2.7. (4R)-2,3-Bis(benzyloxy)-4-hydroxycyclopent-1-ene-ethane-5,6-*O*-isopropylidene

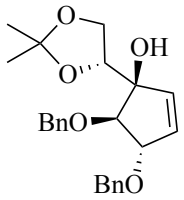

42

To a solution of 2,3-Di-*O*-benzyl-4,4'-didehydro-1,1',4,4'-tetradeoxy-5,6-*O*-isopropylidene-D-galacto-hept-1'-en-4-ol **R-41** (133 mg, 0.312 mmol) in distilled toluene (6.00 mL) was added under an inert atmosphere of argon Hoveyda-Grubbs's second generation catalyst (4 mg, 0.006 mmol, 0.02 equiv.). After 2 h at 80°C. An additional portion of Hoveyda-Grubbs's second generation catalyst (2 mg, 0.003 mmol, 0.01 equiv.) was added to the reaction mixture. After 1 h at the same temperature, the solvent was then concentrated in vacuo to afford a black oil. The resulting residue was purified by column chromatography (Cy/EtOAc 99:1 until 80:20) to afford product **42** (0.86 g, 87 %).

- **Chemical formula:** $C_{24}H_{28}O_5$
- **Molecular weight:** 396.48 g/mol
- **Rf:** 0.17 (Cy/EtOAc 80:20)
- **Aspect:** Brown oil
- **^{1}H NMR (400 MHz, Chloroform-*D*):** δ 7.39 – 7.33 (m, 10H, H arom), 6.06 (dd, *J* = 6.3, *J* = 1.7 Hz, 1H, H-1), 5.96 (dd, *J* = 6.3, *J* = 1.4 Hz, 1H, H-4'), 4.75 (s, 2H, C*H*$_2$Ph), 4.68 (dt, *J* = 3.8, *J* = 1.5 Hz, 1H, H-2), 4.62 (d, *J* = 11.7 Hz, 1H, C*H*$_2$Ph), 4.55 (d, *J* = 11.8 Hz, 1H, C*H*$_2$Ph), 4.13 (dd, *J* = 6.9 , *J* = 5.5 Hz, 1H, H-5), 4.03 (d, *J* = 3.9 Hz, 1H, H-6a), 4.01 (d, *J* = 0.8 Hz, 1H, H-3), 3.99 (d, *J* = 2.2 Hz, 1H, H-6b), 3.23 (s, 1H, OH), 1.42 (s, 3H, CH_3), 1.34 (s, 3H, CH_3) ppm.
- **^{13}C NMR (101 MHz, Chloroform-*D*):** δ 138.2 (Cq arom.), 137.8 (Cq arom.), 134.4 (C-4'), 134.2 (C-1), 129.9 – 126.2 (m, C-H arom.), 109.9 ($C(CH_3)_2$), 87.7 (C-2), 83.5 (C-3), 81.5 (C-4), 78.3 (C-5), 73.3 (CH_2Ph), 71.7 (CH_2Ph), 65.6 (C-6), 26.6 (CH_3), 25.0 (CH_3) ppm.
- **HRMS (ESI):** m/z calculated for $C_{24}H_{28}O_5$ $[M+Na]^+$: 419.1829; 419.1825; δ = 0.9 ppm.

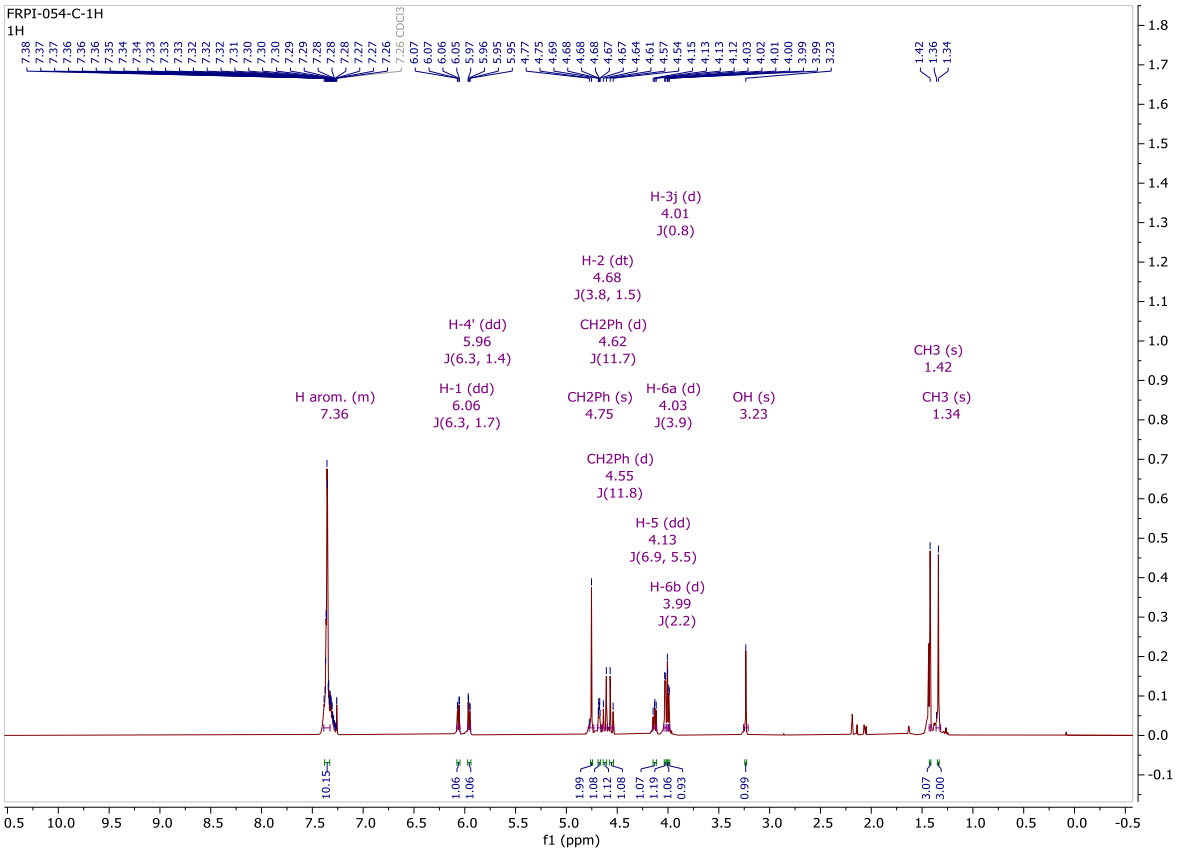
FRPI-054-C-1H
1H
H-3j (d)
4.01
J(0.8)
H-2 (dt)
4.68
J(3.8, 1.5)
H-4' (dd)
5.96
J(6.3, 1.4)
CH2Ph (d)
4.62
J(11.7)
CH3 (s)
1.42
H arom. (m)
7.36
H-1 (dd)
6.06
J(6.3, 1.7)
CH2Ph (s)
4.75
H-6a (d)
4.03
J(3.9)
OH (s)
3.23
CH3 (s)
1.34
CH2Ph (d)
4.55
J(11.8)
H-5 (dd)
4.13
J(6.9, 5.5)
H-6b (d)
3.99
J(2.2)
f1 (ppm)

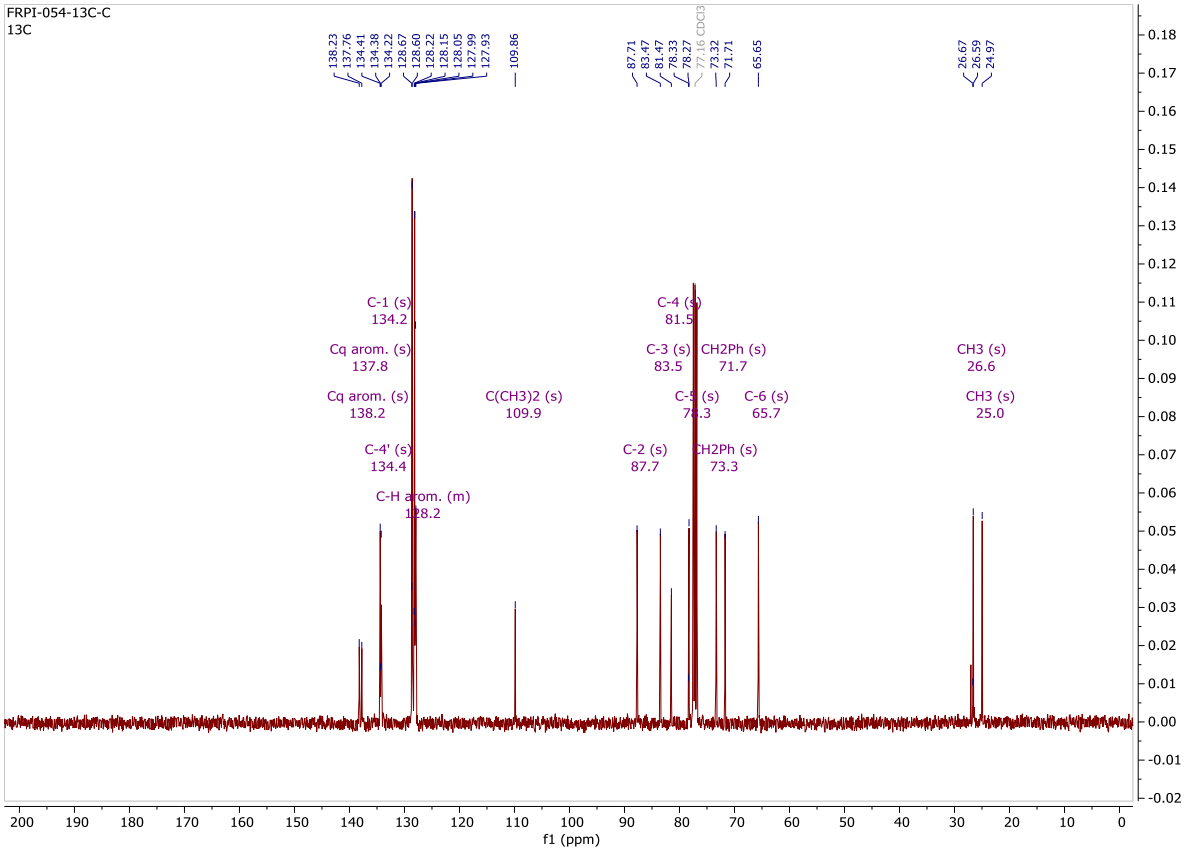
FRPI-054-13C-C
13C
C-1 (s)
134.2
Cq arom. (s)
137.8
Cq arom. (s)
138.2
C-4' (s)
134.4
C-H arom. (m)
128.2
C(CH3)2 (s)
109.9
C-4 (s)
81.5
C-3 (s)
83.5
CH2Ph (s)
71.7
C-6 (s)
65.7
C-2 (s)
87.7
CH2Ph (s)
73.3
CH3 (s)
26.6
CH3 (s)
25.0
f1 (ppm)

VII. BIBLIOGRAPHY

1. Getahun, H., Matteelli, A., Chaisson, R. E. & Raviglione, M. Latent Mycobacterium tuberculosis Infection. *New England J. of Med.* **2015**, *372*, 2127–2135.

2. World Health Organization. Tuberculosis. https://www.who.int/fr/news-room/fact-sheets/detail/tuberculosis (2021).

3. Campbell, E. A. *et al.* Structural Mechanism for Rifampicin Inhibition of Bacterial RNA Polymerase. *Cell.* **2001**, *104*, 901–912.

4. Zimhony, O., Cox, J. S., Welch, J. T., Vilchèze, C. & Jacobs, W. R. Pyrazinamide inhibits the eukaryotic-like fatty acid synthetase I (FASI) of Mycobacterium tuberculosis. *Nat. Med.* **2000**, *6.*

5. Slayden, R. A. & Barry, C. E. The genetics and biochemistry of isoniazid resistance in Mycobacterium tuberculosis. *Microb. and infections* **2000,** *2*, 659–669.

6. Basak, S., Singh, P. & Rajurkar, M. Multidrug Resistant and Extensively Drug Resistant Bacteria: A Study. *J. Pathog.* **2016**, *2016*, 1–5.

7. Ahmad, S. Pathogenesis, immunology, and diagnosis of latent mycobacterium tuberculosis infection. *Clin. Dev. Immunol.* **2011**, *2011*.

8. Pfyffer, G. E. *Mycobacterium:* General Characteristics, Laboratory Detection, and Staining Procedures. in *Manual of Clinical Microbiology* 536–569 (ASM Press, 2015)

9. Nunes-Alves, C. *et al.* In search of a new paradigm for protective immunity to TB. *Nat. Rev. Microbiol.* **2014**, *12*, 289–299.

10. Brown, L., Wolf, J. M., Prados-Rosales, R. & Casadevall, A. Through the wall: Extracellular vesicles in Gram-positive bacteria, mycobacteria and fungi. *Nat. Rev. Microbiol.* **2015**, *13*, 620–630.

11. Vollmer, W., Blanot, D. & de Pedro, M. A. Peptidoglycan structure and architecture. *FEMS Microbiol. Rev.* **2008**, *32*, 149–167.

12. Batt, S. M., Burke, C. E., Moorey, A. R. & Besra, G. S. Antibiotics and resistance: the two-sided coin of the mycobacterial cell wall. *Cell Surf.* **2020**, *6*.

13. Abrahams, K. A. & Besra, G. S. Synthesis and recycling of the mycobacterial cell envelope. *Curr. Opin. Microbiol.* **2021**, *60*, 58–65.

14. Lambert, P. A. Cellular impermeability and uptake of biocides and antibiotics in Gram-positive bacteria and mycobacteria. *J. of Appl. Microbiol. Symp. Supp.* **2002**, *92*, 46–54.

15. Iii, C. E. B. *et al.* Mycolic acids: Structure, Biosynthesis and physiological functions. *Prog. Lipid Res.* **1998**, *37*, 143–179.

16. Dulberger, C. L., Rubin, E. J. & Boutte, C. C. The mycobacterial cell envelope — a moving target. *Nat. Rev. Microbiol.* **2020**, *18*, 47–59.

17. Yuan, Y., Crane, D. C., Musser, J. M., Sreevatsan, S. & Barry, C. E. MMAS-1, the Branch Point Between cis-and trans-Cyclopropane-containing Oxygenated Mycolates in Mycobacterium tuberculosis. *J. of Biol. Chem.* **1997**, *272*, 10041–10049.

18. Brennan, P. 1. The Envelope of Mycobacteria. *Annu. Rev. Biochem.* **1995**, *64*, 29–63.

19. Kieser, K. J. & Rubin, E. J. How sisters grow apart: Mycobacterial growth and division. *Nat. Rev. Microbiol.* **2014**, *12*, 550–562.

20. Abrahams, K. A. & Besra, G. S. Mycobacterial cell wall biosynthesis: A multifaceted antibiotic target. *Parasitology* **2018**, *145*, 116–133.

21. Shen, L. *et al.* The endogenous galactofuranosidase GlfH1 hydrolyzes mycobacterial arabinogalactan. *J. of Biol. Chem.* **2020**, *295*, 5110–5123.

22. Elferink, H., Bruekers, J. P. J., Veeneman, G. H. & Boltje, T. J. A comprehensive overview of substrate specificity of glycoside hydrolases and transporters in the small intestine: "A gut feeling". *Cell. and Mol. Life Sci.* **2020**, *77*, 4799–4826.

23. Callewaert, L. *et al.* Guards of the great wall: bacterial lysozyme inhibitors. *Trends in Microbiol.* **2020**, *20*, 501–510.

24. Cerqueira, N., Brs, N., Joo, M. & Alexandrino, P. Glycosidases – A Mechanistic Overview. in *Carbohydrates - Comprehensive Studies on Glycobiology and Glycotechnology* (InTech, 2012).

25. Sullivan, S. M. & Holyoak, T. Enzymes with lid-gated active sites must operate by an induced fit mechanism instead of conformational selection. *PNAS* **2008**, *105*, 13829-13834.

26. Speciale, G., Thompson, A. J., Davies, G. J. & Williams, S. J. Dissecting conformational contributions to glycosidase catalysis and inhibition. *Curr. Opin. Struct. Biol.* **2014**, *28*, 1–13.

27. Vasella, A., Davies, G. J. & Böhm, M. Glycosidase mechanisms. *Curr. Opin. Chem. Biol.* **2002**, *6*, 619–629.

28. Zechel, D. L. & Withers, S. G. Glycosidase Mechanisms: Anatomy of a Finely Tuned Catalyst. *Acc. Chem. Res.* **2000**, *33*, 11–18.

29. Mccarter, J. D. & Withers, S. G. *Mechanisms of enzymatic glycoside hydrolysis*. *Curr. Opin. in Struct. Biol.* **1994**, *4.*

30. Ren, W. *et al.* Revealing the mechanism for covalent inhibition of glycoside hydrolases by carbasugars at an atomic level. *Nat. Commun.* **2018**, *9*.

31. Rempel, B. P. & Withers, S. G. Covalent inhibitors of glycosidases and their applications in biochemistry and biology. *Glycobiology* **2008**, *18*, 570–586.

32. Street, I. P., Kempton, J. B. & Withers', S. G. Inactivation of a Glucosidase through the Accumulation of a Stable 2-Deoxy-2-fluoro-a-D-glucopyranosy-Enzyme Intermediate: A Detailed Investigation. *Biochem.* **1992**, *31*, 9970–9978.

33. Wu, L. *et al.* An overview of activity-based probes for glycosidases. *Curr. Opin. Chem. Biol.* **2019**, *53*, 25–36.

34. Kallemeijn, W. W., Witte, M. D., Wennekes, T. & Aerts, J. M. F. G. Mechanism-based inhibitors of glycosidases: Design and applications. *Adv. Carbohydr. Chem. Biochem.* **2014**, *71*, 297–338.

35. Caron, G. & Withers, S. G. Conduritol Aziridine: a new mechanism-based Glucosidase Inactivator. *Biochem. Biophys. Res. Commun.* **1989**, *163*, 495–499.

36. Artola, M. *et al.* 1,6-Cyclophellitol Cyclosulfates: A New Class of Irreversible Glycosidase Inhibitor. *ACS Cent. Sci.* **2017**, *3*, 784–793.

37. Kallemeijn, W. W. *et al.* Novel Activity-Based Probes for Broad-Spectrum Profiling of Retaining β-Exoglucosidases In Situ and In Vivo. *Angew. Chem.* **2012**, *124*, 12697–12701.

38. Willems, L. I. *et al.* Potent and selective activity-based probes for GH27 human retaining α-galactosidases. *J. Am. Chem. Soc.* **2014**, *136*, 11622–11625.

39. Schröder, S. P. *et al.* A Divergent Synthesis of l-arabino- and d-xylo-Configured Cyclophellitol Epoxides and Aziridines. *Eur. J. Org. Chem.* **2016**, *2016*, 4787–4794.

40. Artola, M. *et al.* Direct Stereoselective Aziridination of Cyclohexenols with 3-Amino-2-(trifluoromethyl)quinazolin-4(3H)-one in the Synthesis of Cyclitol Aziridine Glycosidase Inhibitors. *Eur. J. Org. Chem.* **2019**, *25*, 1397–1404.

41. El Bkassiny, S. & Vincent, S. The Synthesis of carbasugars via Ring Closing Metathesis Applied to the inhibition of M. Tuberculosis Cell Wall Biosynthesis. *Chimie Nouvelle* **2013**, *114*, 5–10.

42. El Bkassiny, S., N'Go, I., Sevrain, C. M., Tikad, A. & Vincent, S. P. Synthesis of a novel UDP-carbasugar as UDP-galactopyranose mutase inhibitor. *Org. Lett.* **2014**, *16*, 2462–2465.

43. De Talancé, V. L. *et al.* A simple synthesis of D-galactono-1,4-lactone and key building blocks for the preparation of galactofuranosides. *J. Carbohydr. Chem.* **2011**, *30*, 605–617.

44. Massinon, O. Synthèse de glycosides de conformation contrainte en vue de l'inhibition d'hexosaminidases (Thesis), Université de Namur, **2015**

45. Inoue, K., Kitahara, K. I., Aikawa, Y., Arai, S. & Masuda-Hanada, T. Hplc separation of all aldopentoses and aldohexoses on an anion-exchange stationary phase prepared from polystyrene-based copolymer and diamine: The effect of naoh eluent concentration. *Molecules* **2011**, *16*, 5905–5915.

46. Ueberschär, K. -H., Blachnitzky, E. -O. & Kurz, G. Reaction Mechanism of d-Galactose Dehydrogenases from Pseudomonas saccharophila and Pseudomonas fluorescens Formation and Rearrangement of Aldono-1,5-lactones. *Eur. J. Biochem.* **1974**, *48*, 389–405.

47. Yin, B., Ye, D. N., Yu, K. H. & Liu, L. X. A general and simple diastereoselective reduction by l-selectride: Efficient synthesis of protected (4s,5s)-dihydroxy Amides. *Molecules* **2010**, *15*, 2771–2781.

48. Dess, D. B. & Martin, J. C. A Useful 12-1-5 Triacetoxyperiodinane (the Dess-Martin Periodinane) for the Selective Oxidation of Primary or Secondary Alcohols and a Variety of Related 12-1-5 Species'". *J. Am. Chem. Soc.* **1991**, *113*, 7277–7287.

49. Hérisson, J.-L. & Chauvin, Y. Catalyse de transformation des oléfines par les complexes du tungstène. II. Télomérisation des oléfines cycliques en présence d'oléfines acycliques. *Die Makromol. Chem.* **1971**, *141*, 161–176.

50. Zukowska, K., Szadkowska, A. & Grela, K. Olefin Metathesis. in *Comprehensive Inorganic Chemistry II (Second Edition): From Elements to Applications* vol. 6 105–126 (Elsevier Ltd, 2013).

51. Qadir, T., Amin, A., Sarkar, D. & Sharma, P. K. A Review on Recent Advances in the Synthesis of Aziridines and their Applications in Organic Synthesis. *Curr. Org. Chem.* **2021**, *25*, 1868–1893.

52. Nayak, Y. N. *et al.* Chloramine-T (N-chloro-p-toluenesulfonamide sodium salt), a versatile reagent in organic synthesis and analytical chemistry: An up to date review. *J. of Saudi Chem. Soc.* **2022**, *26*, 101416.

53. Mordini, A. *et al.* Base-promoted elaboration of aziridines. *Tetrahedron* **2002**, *58*, 7153–7163.

54. Atkinson, R. S., Grimshire, M. 3 & Kelly, B. J. Aziridination by oxidative addition of E-aminoquinazolones to alkenes: evidence for non-involvement of nitrenes. *Tetrahedron* **1989**, *45*, 2875–2886.

55. Jiang, J. *et al.* Comparing Cyclophellitol N-Alkyl and N-Acyl Cyclophellitol Aziridines as Activity-Based Glycosidase Probes. *Chemistry - A Eur. J.* **2015**, *21*, 10861–10869.

56. Krippendorff, B. F., Neuhaus, R., Lienau, P., Reichel, A. & Huisinga, W. Mechanism-based inhibition: Deriving kiand kinact directly from time-dependent ic50 values. *J. Biomol. Screen.* **2009**, *14*, 913–923.